



***INTERCOMPARISON OF MEDICAL IMAGE
SEGMENTATION ALGORITHMS***

Mamata Naik

2005-2006

A thesis submitted to the Department of Bioengineering
in partial fulfillment of the requirements for the
degree of Master of Science

“Dedicated to my parents”

Declaration

I, Mamata Naik, declare that the work set out in this thesis is essentially my own work and no part of this work has been submitted for a degree at any other academic institution.

Mamata Naik

Strathclyde, September 2006

Abstract

Magnetic Resonance Imaging (MRI) is one of the most widely-used high quality imaging techniques, especially for brain imaging, compared to other techniques such as computed tomography and x-rays, mainly because it possesses better soft tissue contrast resolution. There are several stages involved in analyzing an MRI image, segmentation being one of the most important. Image segmentation is essentially the process of identifying and classifying the constituent parts of an image, and is usually very complex. Unfortunately, it suffers from artefacts including noise, partial volume effects and intensity inhomogeneities. Brain, being a very complicated structure, its precise segmentation is particularly necessary to delineate the borders of anatomically distinct regions and possible tumors. Many algorithms have been proposed for image segmentation, the most important being thresholding, region growing, and clustering methods such as k-means and fuzzy c-means algorithms. The main objective of this project was to investigate a representative number of different algorithms and compare their performance. Image segmentation algorithms, including thresholding, region growing, morphological operations and fuzzy c-means were applied to a selection of simulated and real brain MRI images, and the results compared. The project was realized by developing algorithms using the popular Matlab[®] software package. Qualitative comparisons were performed on real and simulated brain images, while quantitative comparisons were performed on simulated brain images, using a variety of different parameters, and results tabulated. It was found that the fuzzy c-means algorithm performed better than all the other algorithms, both qualitatively and quantitatively. After comparing the performance of all algorithms, it was concluded that, by combining one or two basic algorithms, a more effective algorithm could be developed for image segmentation that is more robust to noise, considers both intensity and spatial characteristics of an image, and which is computationally efficient.

Acknowledgements

I would like to thank my supervisor Prof William Sandham, for his contribution of the expert knowledge to the project and his help has been invaluable.

I would like to thank my family and friends back home for their support and advice. I would like to thank my friend Subrahmanya who has always been a constant source of inspiration and who made my life easy despite the busy schedule during the dissertation work. I would also like to thank my friends Rakesh and Amit for their input and help which they gave me throughout the project.

Last but not the least I would like to thank members of the Bioengineering and EEE Department, University of Strathclyde for use of their laboratories during my work.

TABLE OF CONTENTS

Declaration	iii
Abstract	iv
Acknowledgements	v
TABLE OF CONTENTS	0
Chapter 1	2
Introduction	2
1.1 Motivation.....	2
1.2 Aims and Objectives	3
1.3 Thesis Overview	3
Chapter 2	5
Magnetic Resonance Imaging	5
2.1 Introduction.....	5
2.2 The Basic Principles of MRI.....	5
2.3 MRI Parameters	8
2.4 Artefacts in MRI Images.....	9
2.4.1 RF Quadrature.....	10
2.4.2 RF Inhomogeneity	10
2.4.3 Partial Volume	11
2.4.4 Motion.....	11
2.4.5 Noise	12
2.4.6 Gibbs' Ringing.....	13
2.5 Synthetic MRI Images	13
Chapter 3	15
MRI Image Pre-Processing	15
3.1 Introduction.....	15
3.2 Image Standardization	16
3.3 Morphological Operators	18
3.3.1 Structuring Elements (SE)	18
3.3.2 Erosion	19
3.3.3 Dilation	19
3.3.4 Opening and Closing Morphological Operators	19

3.4 Removal of Non-Brain Regions using Morphological Operators	21
3.5 Tissue Contrast Enhancement.....	22
3.5.1 Histogram Equalization	23
3.5.2 Tissue Contrast Enhancement in MRI Images.....	25
Chapter 4	26
Image Segmentation.....	26
4.1 Introduction.....	26
4.2 Image Segmentation Techniques	26
4.2.1 Thresholding	27
4.2.2 Region Growing.....	30
4.2.3 Edge Based Segmentation.....	32
4.2.4 Morphological Operators- Watershed Transformation Algorithms	33
4.2.5 Clustering.....	36
4.2.6 K-Means Clustering.....	37
4.3 Fuzzy C Means Clustering.....	38
Chapter 5	41
Results	41
5.1 Introduction.....	41
5.2 Results – Non-Brain Region Removal.....	42
5.3 Results using Simulated Images - Image Segmentation Algorithms.....	44
5.4 Results Using Real Images- Image Segmentation Algorithms.....	59
5.5 Comparison of Image Segmentation Algorithms	62
5.5.1 A Qualitative Comparison of Image Segmentation Algorithms.....	62
5.5.2 A Quantitative Comparison of Image Segmentation Algorithms.....	63
Chapter 6	65
Conclusions and Future Work.....	65
References.....	70
APPENDIX I Glossary	73
APPENDIX II Matlab® Functions.....	75
APPENDIX III Source Code for Image Segmentation Algorithms	77
APPENDIX IV COTENTS OF CD.....	79
APPENDIX V A Short Note on the Project Work.....	80

Chapter 1

Introduction

1.1 Motivation

For many years now, physicians have been producing and analyzing medical images using different imaging modalities. Today, highly sophisticated medical imaging modalities are employed regularly in hospitals, which aid considerably in obtaining fast and accurate results. Ultrasound, computed tomography (CT) and magnetic resonance imaging (MRI) are some of the most popular modalities, and use computers and sophisticated algorithms to produce images.

Since the advent of computer image processing, researchers have been seeking ways to classify objects in an image, and study the relationship between objects. Image segmentation is possibly the single most important area of image analysis research being carried out today, and may be defined as the separation of an image into its constituent regions, each having its own property, for example average gray level or texture. It is usually the first step in a process leading to the description, classification and interpretation of an image by higher level processes. Image segmentation techniques have been studied among numerous scientific fields such as pattern recognition, computer vision systems, and medical imaging. In particular, segmentation appears to be a key issue in modern medical image analysis enabling numerous clinical applications, such as three-dimensional (3D) visualization of separate neural structures in magnetic resonance (MR) images, reconstruction of anatomical models, and volumetric analysis of MR images. More recently, image guided radiotherapy treatment planning (IGRT), which involves the use of accurate and sophisticated segmentation algorithms, is one of the most exciting

Intercomparison of image segmentation algorithms techniques to evolve in external beam radiotherapy treatment, since conformal therapy was introduced in the 1990s.

MRI is an important diagnostic imaging technique for early detection of abnormal changes in tissues and organs, and possesses good contrast resolution for soft tissues. Hence, it is more advantageous for brain studies compared to CT. Therefore, considerable research in medical image brain segmentation concerns MR images. The study of brain MRI has become very important because of the complex nature of the brain. Indeed, segmentation of brain structures from MRI is applied to the study of many disorders including multiple sclerosis, schizophrenia, epilepsy, Parkinson's disease, Alzheimer's disease, and cerebral atrophy, amongst others. Additionally, MRI segmentation is an important image processing step to identify anatomical areas of interest for diagnosis, treatment, surgical planning, image registration and functional mapping. The application of image segmentation to brain MRI images has motivated the origins and development of this thesis.

1.2 Aims and Objectives

The primary goal of this thesis was to investigate a representative number of different algorithms for image segmentation and compare their performance. In order to achieve this objective, a Matlab[®] package was used to develop the necessary algorithms. A variety of synthetic and real images were employed for qualitative and quantitative assessment of the algorithms.

1.3 Thesis Overview

This thesis starts with an introduction to the basic physics of MRI in Chapter 2. The basic principles of MRI are discussed briefly, and different MRI parameters involved in the acquisition of various brain images and artefacts (typical artefacts) are discussed. The chapter concludes with a discussion on synthetic brain MRI images. In this work, synthetic brain MRI images were used as an image database to test and compare the various algorithms.

Chapter 3, which is titled ‘MRI Image Pre-Processing’, presents the different kinds of image pre-processing strategy, which include standardization of the intensity scales in MRI images, tissue contrast enhancement, and non-brain region removal using morphological operators. The different kinds of morphological operators like erosion and dilation are discussed in detail.

Chapter 4 is titled ‘Image Segmentation’. In this chapter, the role of image segmentation in image processing is discussed. Image segmentation algorithms like thresholding, region growing, edge based segmentation, watershed algorithms and the fuzzy clustering methods are also discussed in detail. Matlab[®] code was created for a representative number of these algorithms, and this was later tested on brain MRI images.

Chapter 5 is titled ‘Results’, and presents all the results obtained for the various image segmentation algorithms. Algorithms were tested on both simulated and real brain MRI images using a variety of parameters. Both qualitative and quantitative comparisons were performed in order to rank their performance.

Chapter 6 presents conclusions and suggestions for future work.

There are four appendices. Appendix I is the glossary. Appendix II represents the important Matlab[®] functions that were used to develop algorithms. Appendix III includes Matlab[®] source code. Appendix IV is a short summary on the overall work carried out in this thesis.

Chapter 2

Magnetic Resonance Imaging

2.1 Introduction

Magnetic Resonance Imaging (MRI), formerly referred to as Nuclear Magnetic Resonance (NMR), is an imaging modality that is widely used to diagnose different pathological and physiological alterations in the human body. In 1946, two scientists Bloch and Edward Purcell from the United States, discovered the magnetic resonance phenomenon independently and were awarded the Nobel prize for their work in 1952^{42,43}. However, MRI was tested on human beings only after 1977. Since then, faster computing has made the MRI process much faster. Paul C. Lauterbur and Peter Mansfield carried out work in MRI for many years and were awarded the Nobel Prize in 2003 for their discoveries of using MRI as a diagnostic tool⁴¹. Today, most hospitals worldwide use MRI scanners as a medical diagnostic tool, and scientists are now working on MRI to make it a more efficient and sophisticated imaging tool. Therefore, it is important for the present context to understand the underlying principles of MRI.

2.2 The Basic Principles of MRI

MRI makes use of the magnetic properties of hydrogen atoms, and their interaction with powerful external magnetic fields and radio waves, to produce a highly detailed image of the human anatomy. Hence, knowledge of the atomic structure of hydrogen atoms is necessary in order to understand the basic principles of MRI.

An atom mainly consists of a neutron and a proton, the proton being positively charged and the neutron being neutral. Neutrons and protons spin around their axes. Electrons carry a negative charge and orbit around not only the nucleus, but also spin about their

Intercomparison of image segmentation algorithms own axis. The spinning of these nuclear particles produces a spin angular momentum and this angular momentum is expressed as a vector quantity. In addition to spin angular momentum, certain nuclei exhibit magnetic properties. Because a proton has mass, a positive charge and spins, it produces a small magnetic field much like a bar magnet. This small magnetic field of the proton is known as the magnetic moment. The magnetic moment is also a vector quantity and is oriented in the same direction as the angular momentum. The ratio between the angular momentum and the magnetic moment is a constant known as the 'gyromagnetic ratio', which is specific to each magnetically active nuclei.¹

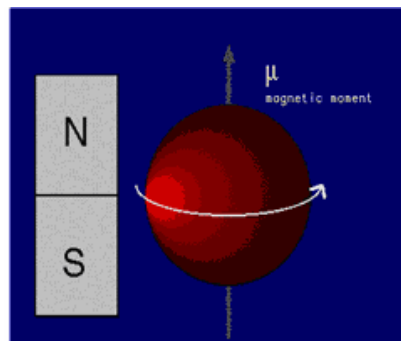


Figure 2.2.1 A magnetic moment created by a spinning nucleus that acts like a bar magnet¹.

The human body is made up chemically of fat and water (mostly), water constituting around 70% of body weight. Both fat and water contain large numbers of hydrogen atoms. Since hydrogen atoms constitute a major part of the body, and their protons have significant magnetic moments, we consider hydrogen atoms in MRI imaging.

The nucleus of hydrogen atoms contains a single proton, and such nuclei containing an odd number of protons and/or neutrons have a characteristic motion or precession. Since nuclei are charged particles, this precession produces a small magnetic moment. When the human body is placed in a large magnetic field of 0.5 to 1.5 Tesla in order to obtain MRI images, hydrogen nuclei align in the direction of the magnetic field and create a net magnetic moment M , parallel to B_0 . This behavior is termed Larmor Precession². This

Intercomparison of image segmentation algorithms
 precessional frequency is proportional to the applied magnetic field strength and is termed the Larmor frequency ω_0 , defined as follows,

$$\omega_0 = \gamma B_0 \quad (2.2)$$

where γ is the gyrometric ratio, which is a nuclei specific constant, and B_0 is the strength of the applied magnetic field. For hydrogen, $\gamma = 42.6$ MHz/Tesla . This is shown in Figures 2.2.2 and 2.2.3².

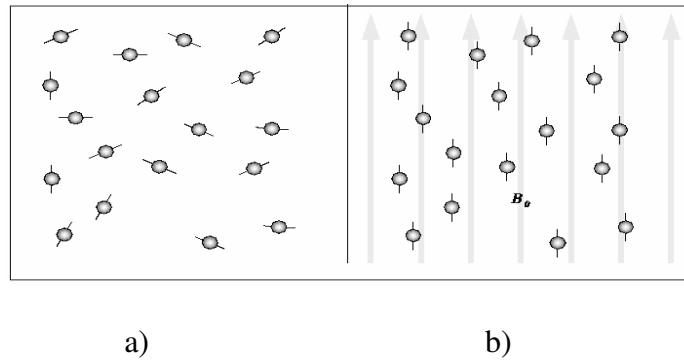


Figure 2.2.2 a) In the absence of the magnetic field, the hydrogen atoms are randomly aligned; b) When a magnetic field, B_0 , is applied the hydrogen nuclei precess about the direction of the field.²

Next, a radio frequency (RF) pulse B_{rf} is applied perpendicular to B_0 . This pulse, with a frequency equal to the Larmor frequency, causes M (Magnetic Moment) to tilt away from B_0 . This is shown in Figure 2.2.3.

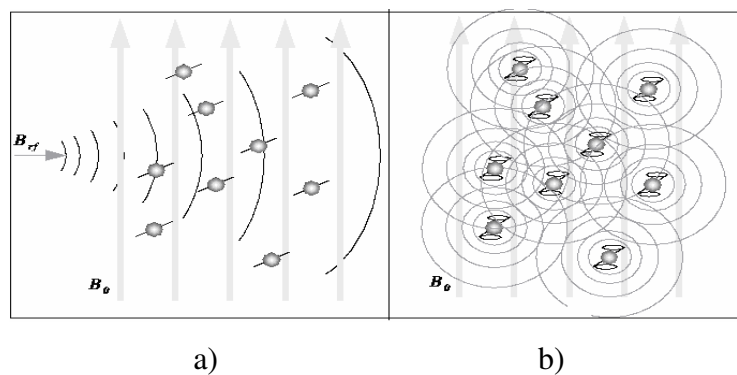


Figure 2.2.3 a) The RF pulse B_{rf} causes the net magnetic moment of the nuclei, M , to tilt away from B_0 . b) When the RF pulse stops, the nuclei return to equilibrium such that M is again parallel to B_0 . During realignment, the nuclei lose energy by generating a measurable RF signal.²

Once the RF signal is removed, the nuclei realign themselves such that their net magnetic moment M , is again parallel with B_0 . This return to equilibrium is referred as relaxation. During relaxation, the nuclei convert their energy by emitting their own RF signal (Figure 2.2.3 b). This signal is referred as the Free Induction Decay (FID) response signal. The FID response signal is measured by a conductive field coil that is placed around the object that has to be imaged. This measurement is processed to obtain 3D grey-scale MR images².

2.3 MRI Parameters

In this section, important parameters of MRI are discussed. These parameters are involved in the generation of different types of MRI images. The basic parameters of MRI are relaxation times (T1, T2), repetition time (TR) and echo time (TE).

When the RF pulse is removed, the hydrogen nuclei convert their energy in a process called relaxation that occurs in both the longitudinal and transversal plane³. Relaxation in the longitudinal plane is the return of the longitudinal magnetization to equilibrium, and is referred as T1 recovery. The hydrogen nuclei emit the energy that was previously acquired by them, and the surrounding tissues absorb this energy. This phenomenon is referred as ‘spin-lattice relaxation’⁴. This occurs exponentially over time, T1 being the time required to recover 63% of the longitudinal magnetization. On the other hand, relaxation in the transverse plane occurs at the same time but is a completely different process. In this case, the loss of transversal magnetization is due to the energy interchange between the neighbouring hydrogen nuclei and is known as spin-spin relaxation or T2 decay. The nuclei which began spinning in the phase when RF was applied lose their

Intercomparison of image segmentation algorithms coherence and spin in a random fashion. This process has an exponential behaviour, T2 being the time when the transverse magnetization is at 37% of the original value. Usually, T2 decay occurs more rapidly than the regrowth of the longitudinal magnetization³.

The amount of T1 recovery that occurs is determined by the repetition time (TR). TR is the time between consecutive RF pulses. The time from the application of the RF pulse to the peak signal in the receiver coil is referred to as echo time (TE). These two parameters determine the type of image that is obtained. T1-weighted image acquisition is obtained with a short TR and a short TE, and T2-weighted images are obtained with a long TE and a long TR. Proton density images (PD) are obtained by minimizing the effects of T1 and T2 times. In this case, a long TR and a short TE are chosen.

For each tissue, T1 and T2 relaxation properties are different. For instance, T1 recovery time for tissues such as fat is short, compared to other substances like water. In PD images, bright tissues correspond to a higher hydrogen nuclei density.

The table below presents the intensities for each tissue related to the type of MRI image.

Tissue/Image type	T1-Weighted	T2-Weighted	PD Weighted
Fat	Bright	Dark	Bright
Cyst	Dark	Bright	Dark
White Matter	Bright	Grey	Grey
Gray Matter	Grey	Bright	Bright
CSF	Dark	Bright	Grey

Table 2.3 Brightness of tissues for different MRI images⁴.

2.4 Artefacts in MRI Images

An artefact (noise) in an image is a feature that is not present in the original image. In a MRI image, various factors contribute to the appearance of artefacts. Some of them affect the quality of the image, whereas others may be confused with pathologies⁵. For instance,

RF inhomogeneity is reflected as an intensity variation across the image and is produced by a non-uniform magnetic field or a sensitivity variation in the receiver coil⁴. This variation has a considerable drawback when image segmentation is intended. Other artefacts may appear due to the movement of the patient during the scanning process resulting in blurring of the entire image. Noise in MRI images affect the quality of the image, and hence precise results are difficult to obtain. This in turn leads to false diagnosis.

Artefacts are typically classified according to their source. A few of these are discussed below.

2.4.1 RF Quadrature

This artefact is due to the problem with RF detecting circuitry. These problems are caused due to the improper functioning of detectors. For example, if one of the amplifiers consists of a DC offset in its output, then the Fourier transformed data can display a bright spot in the center of the image. If one channel of the detector has a higher gain than the other it will result in ghosting of objects diagonally in the image. This artefact is the result of a hardware failure and must be addressed by a technical service representative.

2.4.2 RF Inhomogeneity

MRI assumes a homogenous B_0 (magnetic field). Inhomogeneity in B_0 can cause distorted images. These distortions can be either spatial, intensity based, or both. Intensity distortions result from the field homogeneity in a location being greater or less than that in the rest of the imaged object. The T2 in this region is different, and therefore the signal will tend to be different. Spatial distortion results from long-range field gradient in B_0 that is constant. They cause spins to resonate at Larmor frequencies other than those prescribed by an imaging sequence.

2.4.3 Partial Volume

Partial volume is an artefact caused by the size of a voxel in an image. For example, if a small voxel contains only a fat or water signal, and a larger voxel contains a combination of the two, the larger voxel will possess signal intensity equal to the weighted average of the quantity of water and fat present in the voxel. Another manifestation of this type of artefact is a loss of resolution caused by multiple features present in the image voxel. The partial volume effect is particularly noticeable in the extreme slices of MRI volumes. Figure 2.4.3 below, shows the first and the last slice of a PD-Weighted MRI image. Figure 2.4.3 a) is the first slice of the PD-Weighted image, the lower right corner of this image appears dim because the tissues below the brain contribute to the intensity of the slice. The arrow in the figure points towards the dim part in the slice. Figure 2.4.3 b) shows the last slice of the PD-Weighted image. The boundary of the brain is blurred because the voxels in that area represent both the brain and the Cerebral Spinal Fluid (CSF). The arrow in the figure shows the region which is blurred.

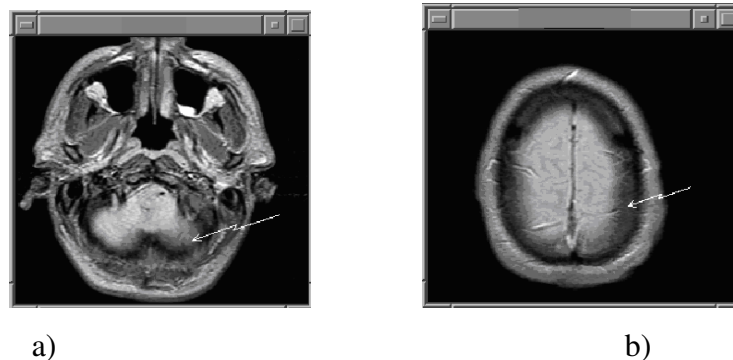


Figure 2.4.3 Partial volume effect. The arrow in the figure a) shows the dim brain tissues. Arrow in b) shows blurred part in the image ².

2.4.4 Motion

Motion artefacts may be caused by the motion of the patient or imaged objects. Motion artefacts can cause blurring of an image.

2.4.5 Noise

During phase encoding, information is obtained in the frequency domain, so the signal is expressed as,

$$Z(u, v) = Z_{re}(u, v) + i Z_{im}(u, v) \quad (2.4.5.1)$$

where $Z(u, v)$ is the signal in the frequency domain, the first term being its real part and the second term being the imaginary part. The variables u and v represent the horizontal and vertical spatial frequencies, and $i = \sqrt{-1}$. This signal can be expressed as follows⁷.

$$Z(u, v) = S(u, v) + N(u, v) \quad (2.4.5.2)$$

where, $S(u, v)$ is the noise-free MRI signal and $N(u, v)$ is complex white Gaussian noise, due to the thermal noise in the patient. A Fast Fourier Transform (FFT) is applied to the final image. Phase errors cause the inverse FFT to be complex. Thus, the signal obtained is,

$$z(m, n) = [s(m, n) \cos(\theta(m, n)) + n_{re}(m, n)] + i[s(m, n) \sin(\theta(m, n)) + n_{im}(m, n)] \quad (2.4.5.3)$$

As observed, both the real and the imaginary channels are now random variables with variance σ^2 , where $\theta(m, n)$ is the phase error as mentioned above. Due to this error, the magnitude of this signal is used to reconstruct the MRI image. The employed signal is,

$$|z(m, n)| = ([s(m, n) \cos(\theta(m, n)) + n_{re}(m, n)]^2 + [s(m, n) \sin(\theta(m, n)) + n_{im}(m, n)]^2)^{1/2} \quad (2.4.5.4)$$

The use of magnitude to obtain the MRI image causes the noise distribution to change from Gaussian to Rician, since it is the square root of the sum of two independent Gaussian variables. This was shown in a study⁶. This kind of distribution tends to a Rayleigh distribution when the signal to noise ratio (SNR) is low, whereas for high SNR it tends to a Gaussian distribution. The contribution of Rician noise to MRI images is significant, since it can hide edges or even make discrimination of different tissues impossible.

2.4.6 Gibbs' Ringing

The Gibbs' or ringing artefact appears as a series of lines parallel to a sharp intensity edge in an image. This artefact is due to the Gibbs' phenomenon, which describes an overshoot or ringing of the Fourier series occurring at discontinuities. These fine lines in the image may be due to the undersampling of the high spatial frequencies. This artefact is seen in images when a small acquisition matrix is used. Therefore, the artefact is more pronounced in the 128 point dimension of a 512x128 acquisition matrix. This artefact may be partially removed by using smoothing filters.

2.5 Synthetic MRI Images

In the present work, algorithms were written for image segmentation and non-brain removal. In order to test above developed algorithms, an image source or database of brain MR images was required. These data can be obtained either from an internet\website (simulated or synthetic data), or can be collected from hospital radiology departments (real data).

The web-based MRI simulator ⁷ was chosen as an image database provider in this work. This simulator allows the choice between two types of database, one with normal brain images and the other with multiple sclerosis lesion brain images. In this work, normal brain MRI images were chosen and processed. The parameters that can be configured in these synthetic images include imaging modality (T1, T2, PD), slice thickness (in millimeters), noise percentage (calculated relative to the brightest tissue) and RF inhomogeneity. Moreover, there is an option to choose the preferred map for visualization of the image, including grayscale, hotmetal and spectral. In this work, all processing was carried out in grayscale. These images, which have intensity values ranging from 0 to 255 and sizes of 258 by 258, were retrieved from Brain Web. A typical image for each modality is shown below, with 0% noise and 1mm slice thickness.

Intercomparison of image segmentation algorithms

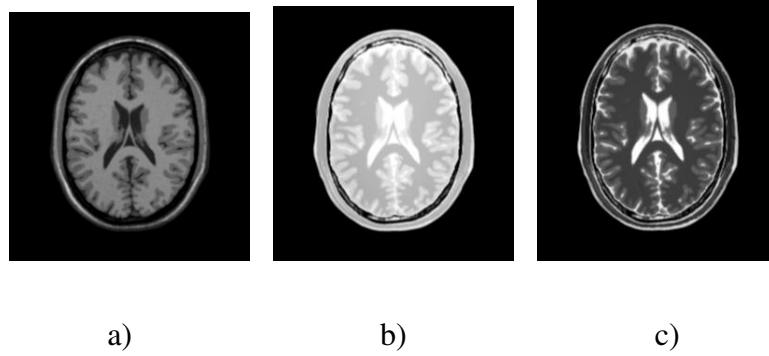


Figure 2.5 a) T1-Weighted Image; b) PD-Weighted Image; c) T2-Weighted Image

Chapter 3

MRI Image Pre-Processing

3.1 Introduction

Image pre-processing plays a pivotal role in image processing, and is performed before segmenting an image. However, it is not the focus of this thesis. Therefore, image pre-processing and its various methods are discussed briefly in this chapter.

Image pre-processing comprises three main steps - image standardization, removal of non-brain region, and contrast enhancement. The MRI images obtained from hospitals usually have non-standard intensity values. Hence, they should not be directly used to perform segmentation. Due to the non-standard intensity values, displaying each MRI image using the same window setup becomes difficult. Hence, interpretation of an image becomes difficult. Therefore, the first and foremost step in image pre-processing is ‘standardization of a MRI image’. Section 3.2 describes the image standardization method and its different types in more detail.

The second step in image pre-processing is non-brain region removal. The brain MR image consists of both brain and non-brain regions. The non-brain region includes skull and meninges. Since image segmentation is performed on tissues of interest in brain regions only, non-brain regions should be excluded from an image before performing any segmentation. This is because non-brain regions may have the same intensity value as the tissues of interest in the brain region. Therefore, non-brain region removal is another important part in image pre-processing. One of the most widely used methods for non-

brain region removal is morphological processing. Section 3.3 explains morphological processing and its various types in detail.

The third step in image pre-processing is tissue contrast enhancement. In order to measure tissue intensities, brain MR images must be segmented into different tissues such as white matter, gray matter, CSF, and possibly brain tumors. High contrast images assist easier segmentation, especially in the segmentation between white and gray matter, which often have similar intensity values and might cause inaccurate image segmentation. Hence, contrast enhancement is an integral part of the image pre-processing step. Section 3.4 describes contrast enhancement techniques in more detail.

3.2 Image Standardization

Image standardization is one of the important steps in image pre-processing. It is observed that MRI images taken from the same patient, using the same MRI scanner, may appear different at different times. The reasons for such variations may be due to scanner dependent variations or parameters, and therefore the absolute dependent values do not have a fixed meaning. Hence, it is necessary to standardize these MRI images by standardizing the intensity scales, so that these intensities are meaningful and comparable⁸.

There are several approaches used to standardize an MRI image. Nyul and Udupa proposed a standardization procedure in 1999⁸. This method comprises two steps: a training step for each MRI image and body region, and a transformation step on each given image. It scales the original MRI images into the same maximum and minimum intensity values. However, this method suffers from one drawback. It cannot be used on MRI images, which include pathological abnormalities, especially in the intensity-based analysis. For example, if MRI images are used to diagnose a brain tumor based on their intensities, and if each image has the same maximum and minimum intensity, then the tumors in different images cannot be represented because they have similar tissue intensities.

A method proposed by Shen ⁴, overcomes the above drawback. This method retains basic intensity features of the images and standardizes the intensity. It makes use of statistical analysis, where the statistical features of the pixel intensities are considered. A brief description of this method is provided below.

The first peak of a MRI image histogram represents the background pixels, which do not provide any useful information and generally occupy 5% of the maximum intensity value in an image. However, this might not hold true for all MRI images. The percentage value may vary from one image to another. Therefore, to achieve accurate results, the value selected was in the range of 1-10% of the maximum intensity value. A new histogram plot was obtained which had only foreground pixels. The next step applies statistical features to the newly obtained histogram. It was found that the intensities of the foreground pixels followed a 'Normal Distribution' function. Hence, the normal distribution function was used to standardize the intensity values for an image. The intensities of foreground pixels were considered as data sets within this normal distribution. The value of 'mean' and 'standard deviation' were computed. The value of the mean and standard deviation are computed by considering one of the important properties of the normal distribution function. This property states that 'About 68% of the values obtained from a normal distribution lie within 1 standard deviation away from the mean and 95% of the values lie within 2 standard deviations away from the mean on its either side'. A set of images were taken and the 'standardized value' of mean and standard deviation were obtained for the foreground signal intensities which could supply best contrast properties for most of the images. The image was then standardized using the 'standardized value' of mean and standard deviation⁴. Figure 3.2(a) shows the original histogram for an MRI image and Figure 3.2(b) shows the final histogram in which the background pixels have been eliminated.

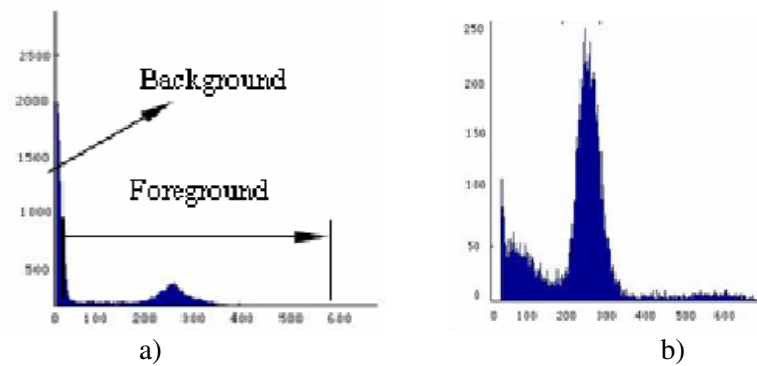


Figure 3.2 a) Original Histogram; b) New histogram of the foreground pixels ⁴.

In this thesis, brain images were normalized based on the concept that was developed by Shen ⁴ for image standardization (normalization). The developed segmentation algorithms were then employed on normalized images.

3.3 Morphological Operators

Non-brain regions such as skull, hair, and meninges in brain MRI images do not provide any useful information and hence should be removed before any segmentation is performed. Morphological processing is one of the commonly used techniques employed in non-brain region removal ^{11, 12}.

Morphological operators are non-linear operators that are useful for identifying or extracting relevant structures from an image. For instance, using morphological operators it is possible to extract the boundaries of an object or even remove parts of it. This consists in moving a known structure called a Structuring Element (SE) through the entire image and setting every pixel to 0 or 1 according to some criterion. Dilation and erosion are the two basic morphological operators, and these form the basis for more complex operations known as Opening and Closing.

3.3.1 Structuring Elements (SE)

The structuring elements are a set of known shapes such as rectangles, squares, and circles. The size and shape of the SE depends on the particular image.

3.3.2 Erosion

This morphological transformation ‘shrinks’ or ‘thins’ objects in an image. In other words, it is used to remove pixels from the boundaries, break connections between objects in an image and increase the number of holes.⁴

If $\mathbf{A} = [\mathbf{a}]$ is the image and \mathbf{B} is a SE with $\mathbf{B} = [\mathbf{b}]$ whose shape is typically a square, a disk or a rectangle, then the erosion of \mathbf{A} by \mathbf{B} is defined as,

$$\mathbf{A} \ominus \mathbf{B} = \{\mathbf{a} \in \mathbf{A} \mid (\mathbf{a} + \mathbf{b}) \in \mathbf{A}, \mathbf{b} \in \mathbf{B}\} \quad (3.3.2)$$

Erosion reduces noise, removes small objects that are of no interest, collapses weak connections between objects, and increases the size of holes by removing the pixels around the perimeter of the holes within the object.

3.3.3 Dilation

Dilation is the opposite of Erosion. It helps to thicken, enlarge objects and fill holes.

If $\mathbf{A} = [\mathbf{a}]$ is the image and \mathbf{B} is a SE with $\mathbf{B} = [\mathbf{b}]$ whose shape is typically a square, a disk or a rectangle, then the dilation of \mathbf{A} by \mathbf{B} is defined as,

$$\mathbf{A} \oplus \mathbf{B} = \{\mathbf{c} \in \mathbf{A} \mid \mathbf{c} \in \mathbf{a} + \mathbf{b}, \mathbf{a} \in \mathbf{A}, \mathbf{b} \in \mathbf{B}\} \quad (3.3.3)$$

In practice, image processing applications make use of various combinations of dilation and erosion operations. Indeed, as mentioned briefly above, the Opening and Closing morphological operators make use of a combination of erosion and dilation operators. These will now be discussed.

3.3.4 Opening and Closing Morphological Operators

If $\mathbf{A} = [\mathbf{a}]$ is the image and \mathbf{B} is a SE with $\mathbf{B} = [\mathbf{b}]$, then the morphological opening of \mathbf{A} by \mathbf{B} , denoted $\mathbf{A} \circ \mathbf{B}$, is simply erosion of \mathbf{A} by \mathbf{B} , followed by the dilation of the result by \mathbf{B} . This is defined formally as

$$\mathbf{A} \circ \mathbf{B} = (\mathbf{A} \ominus \mathbf{B}) \oplus \mathbf{B} \quad (3.3.4.1)$$

An alternative mathematical formulation of Opening is,

$$\mathbf{A} \circ \mathbf{B} = \cup \{ (\mathbf{B})_z \mid (\mathbf{B})_z \subseteq \mathbf{A} \} \quad (3.3.4.2)$$

where $\cup \{ \bullet \}$ denotes the union of all the sets inside the braces, and the notation $C \subseteq D$ means that C is a subset of D . This $\mathbf{A} \circ \mathbf{B}$ formulation has a simple geometric interpretation, as the union of all the translations of \mathbf{B} that fit entirely within \mathbf{A} .

Figure 3.3.4.1 illustrates this interpretation. It shows a set \mathbf{A} which is an image, and \mathbf{B} shows a disk-shaped structuring element^{11, 12}. The translation of \mathbf{B} that fits entirely within \mathbf{A} is as shown. The union of all such translations is also shown in the figure. This region is the complete opening. The white regions in the figure are the areas where the structuring element could not fit completely within \mathbf{A} , and hence are not part of the opening. Opening completely removes the region of the object that does not contain the structuring elements, smooths the object contours, breaks thin connections and removes the protrusions.

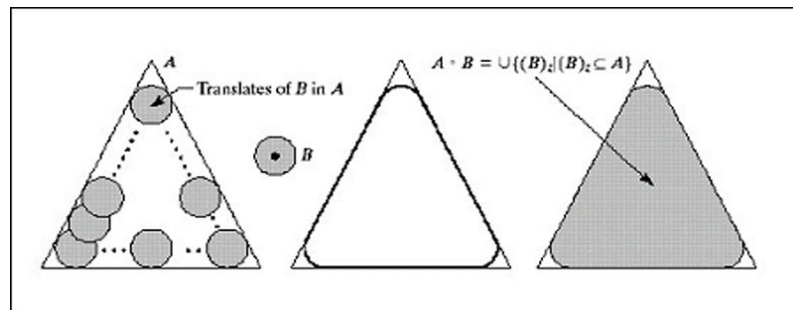


Figure 3.3.4.1 Morphological Opening¹².

The closing of \mathbf{A} by \mathbf{B} , denoted by $\mathbf{A} \bullet \mathbf{B}$, is defined as dilation followed by erosion,

$$\mathbf{A} \bullet \mathbf{B} = (\mathbf{A} \oplus \mathbf{B}) \ominus \quad (3.2.4.3)$$

$\mathbf{A} \bullet \mathbf{B}$ is the compliment of the union of all the translations \mathbf{B} which do not overlap \mathbf{A} . Figure 3.3.4.2 below, illustrates the following. The figure shows the translations of \mathbf{B} that do not overlap \mathbf{A} . By taking the compliment of the union of all such translations, the shaded region is obtained, which is a complete closing.

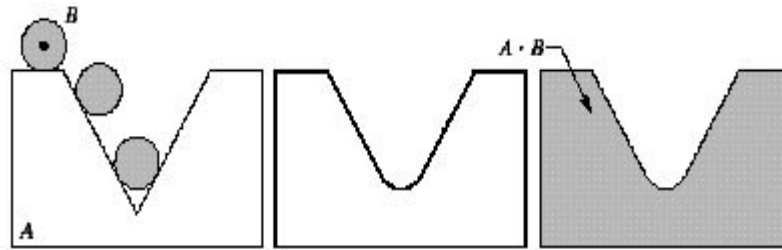


Figure 3.3.4.2 Morphological Closing¹².

3.4 Removal of Non-Brain Regions using Morphological Operators

There always exists a gap between the brain and non-brain regions, which have lower intensities, as compared to other parts in an image. This leads to a dark gap between the non-brain regions and the brain⁴. Morphological operators can be used to separate the brain and non-brain regions.

Morphological operators are usually applied to binary images. When applying to a gray scale image, first a threshold value is selected. This threshold value is used to obtain the binary mask of an image. The optimal value of the threshold can enhance the gap between the non-brain regions and the brain in the binary mask, thereby simplifying removal. As stated above, the distribution of foreground pixel intensities in MR images is a sub-normal distribution; the centre of histogram approximately represents the mean of the intensities, which approaches the intensity value with the maximum number of pixels. As the gap between the non-brain and brain always has lower intensities than the mean, the threshold for the binary mask is chosen practically to be the intensity value corresponding to the maximum number of pixels in the histogram of the foreground pixels. The ideal threshold can enable a binary mask having a pixel value of 0 for the gap and not have connected pixels within it.

The process of non-brain region removal is summarized below.

1. Thresholding: Thresholding is performed in order to obtain a binary image. An intensity value called as a 'threshold' is selected, whose value corresponds to the maximum number of pixels in the histogram (foreground pixel histogram).

2. Erosion: A morphological operator called erosion is applied in order to sever the connections between brain and non-brain regions.
3. Labeling: The objective of labeling is to identify the non-brain regions and isolate them from the brain regions.
4. Dilation: A morphological operation, which is used to recover the brain regions which were thinned down during the erosion operation.
5. Masking removes the dilated non-regions from the original MRI image.

Figure 3.4 shows the non brain region removal in a T1-weighted image.

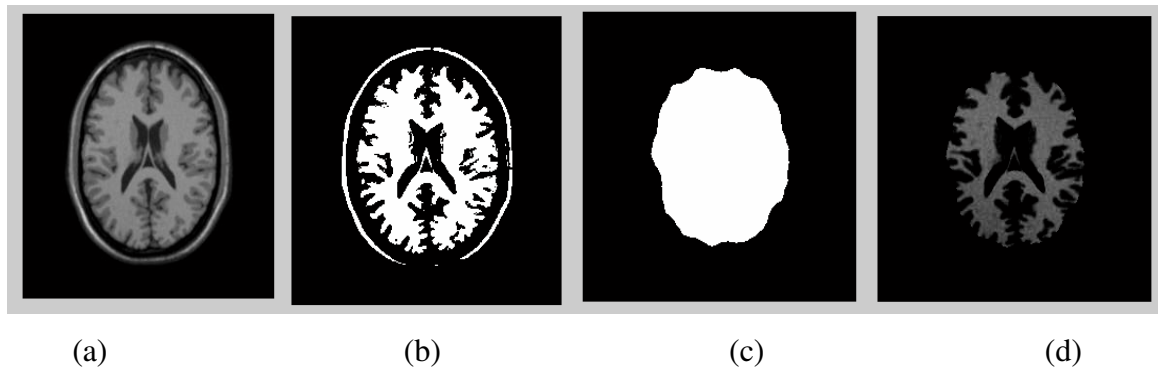


Figure 3.4 a) input image; b) binary image obtained after thresholding; c) mask after morphological operation; d) output image.

3.5 Tissue Contrast Enhancement

In order to measure the tissue intensities, the brain MRI image must be segmented into different tissues such as white matter, grey matter, and CSF. High contrast images enable the segmentation process to be much easier, especially between the white and grey matter, because these have intensity values which are very near one another, and hence contrast enhancement helps in distinguishing these tissues more precisely. Hence, contrast enhancement is one of the essential steps before image segmentation.

Spatial and frequency domain techniques are two types of contrast enhancement techniques. Spatial domain techniques are used for image smoothening, sharpening or averaging. Some spatial domain techniques compute new intensity values for each pixel

Intercomparison of image segmentation algorithms by making use of mathematical operators such as logarithms, exponentials or piecewise-linear transformations. The frequency domain techniques apply the Fourier Transform to the image prior to image manipulation⁸. Other methods such as histogram matching make use of the information contained in the histogram instead of directly operating on the pixels of an image.

3.5.1 Histogram Equalization

Histogram modeling techniques, like histogram equalization, provide a sophisticated method for modifying the dynamic range and the contrast of an image such that its intensity histogram has the desired shape. Histogram equalization employs a monotonic, non-linear mapping, which re-assigns the intensity values of the pixels in the input image, such that the output image contains a uniform distribution of intensities (i.e. a flat histogram). This technique is used in image comparison processes (because it is effective in detail enhancement) and in the correction of non-linear effects.

Ideally, the equalized histogram is a flat histogram. However, in practice a completely flat histogram cannot be obtained. Figures 3.4.1(a) and 3.4.1(b) shows an idealized transformation of an original histogram into an equalized histogram.

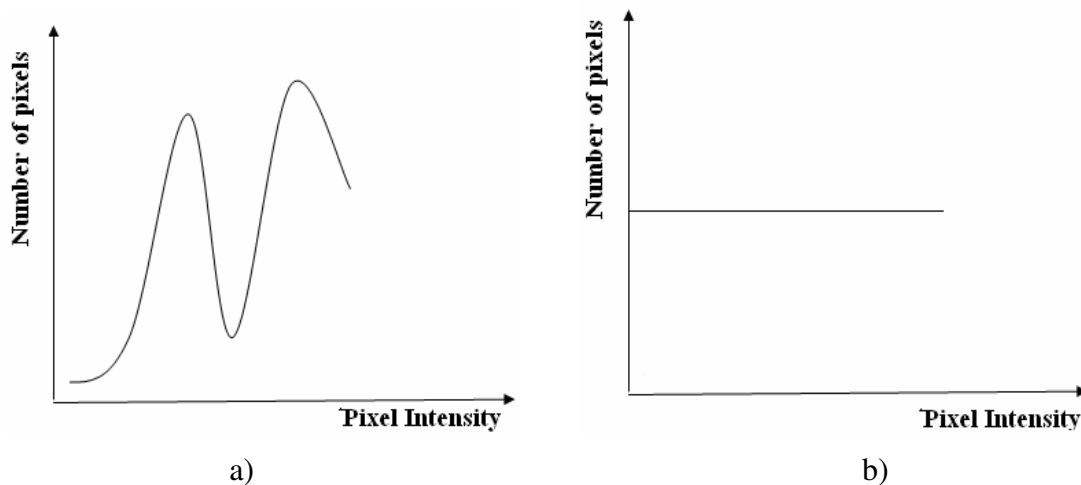


Figure 3.5.1 a) Original histogram; b) Ideal histogram (equalized histogram).

A more detailed explanation of the histogram is provided below.

Consider that r is a variable that represents the gray levels of the image to be enhanced. This variable is continuous and has been normalized to the interval $[0,1]$, where 0 and 1 represent black and white, respectively. Let f denote a function. When this function is applied to the value of r , it produces another set of values s , which are of the form,

$$s = f(r) \quad 0 \leq r \leq 1 \quad (3.5.1.1)$$

As stated above, f monotonically increases in the interval $[0,1]$ and s is a variable whose values are also in the interval $[0,1]$. The gray levels r and s can be viewed as random variables in that interval. One of the most fundamental descriptors of a random variable is its probability density function (PDF). It can be shown that if $p_r(r)$ and f are known, and if f is monotonically increasing in the interval $[0,1]$, then $p_s(s)$ can be obtained as follows:

$$p_s(s) = \frac{p_r(r)}{\left| \frac{df(r)}{dr} \right|} \quad (3.5.1.2)$$

where, $p_r(r)$ is the PDF of r and $p_s(s)$ is the PDF of s . It can be proved⁴ that the transformation function $f(r)$ is of the form

$$s = f(r) = \int_0^r p_r(w) dw \quad (3.5.1.3)$$

where w is the dummy variable of integration, and produces an output image s whose PDF is uniform, $p_s(s)=1$. Generally, the output image has higher contrast and better subjective quality than the original image. For discrete values, the probability of occurrence of gray level r_k is approximated by,

$$p(r_k) = \frac{n_k}{n} \quad k = 1, 2, 3 \dots L-1 \quad (3.5.1.4)$$

where n is the number of pixels, n_k is the number of pixels that have gray level r_k and L is the total number of possible gray levels in the image. The discrete version of the transform is f given by,

$$s_k = f(r_k) = \sum_{j=0}^k \frac{n_j}{n} \quad (3.5.1.5)$$

Thus, a processed output image is obtained by mapping each pixel with the level r_k in the input image into a corresponding pixel with the level s_k in the output image. Note that histogram equalization is applied only to the foreground pixels of the image. Otherwise, the contribution of the background pixels would distort the image.

3.5.2 Tissue Contrast Enhancement in MRI Images

It is observed that in most of the brain MRI image, the gray matter and the white matter in a brain region have similar intensities. This might affect the segmentation results. Therefore, tissue contrast enhancement is very necessary in order that the white and gray matter can be clearly distinguished.

It is observed that the tissue intensities for CSF vary in different MRI images. For example, for T1-Weighted and PD-weighted images, tissues of CSF have the lowest intensities, whereas for T2-weighted it has highest intensities. However, for white and gray matter, the intensities always lie in the middle of the intensity range, for any kind of MRI image. Hence tissue contrast enhancement should be applied only to this middle intensity range in order to clearly distinguish between the gray and white matter.

Chapter 4

Image Segmentation

4.1 Introduction

In general, image segmentation involves partitioning an image into non-overlapping constituent regions that are homogenous with respect to some characteristic such as texture or intensity. The main objective of segmenting an image is to simplify it so that it is more meaningful and easier to analyse. Image segmentation finds applications in different areas. In industrial settings, it's used to analyse the image of the objects in order to detect faults in electronic assemblies such as missing components or faults in the connection paths. Its applications also include areas such as pattern recognition in computer vision and numerous biomedical applications including automated tumour detection, 3-D and multimodal imaging and volumetric segmentation.⁸

In the present work, interest lays in the segmentation of brain MRI images. Today, different kinds of image segmentation technique have been employed to segment brain MRI images, which yield faster and more accurate results compared to traditional segmentation methods like thresholding. Some of the most widely used segmentation methods are thresholding, region growing and clustering. Various research papers^{13, 14, 15} discuss these methods.

4.2 Image Segmentation Techniques

Image segmentation methods may be classified into three main categories:

- 1) Characteristic feature thresholding or clustering.
- 2) Edge detection methods.
- 3) Region oriented techniques.

4.2.1 Thresholding

Thresholding, being one of the oldest image segmentation methods is simple and convenient to use. The thresholding method is most useful when a region of interest that corresponds to an object in an image, has be separated from the region that corresponds to its background. The thresholding method considers the intensity values of the pixels, which is one of the important characteristics in an image. Thresholding involves segmenting the scalar images by creating a binary partitioning of the image intensities.

Mathematically, thresholding is explained by eq.(4.2.1.1) below,

$$S(i,j) = k \text{ if } T_{k-1} \leq f(i,j) < T_k \text{ for } k = 0,1,2,\dots,m-1 \quad (4.2.1.1)$$

where i, j = Co-ordinates of the pixels in the x and y directions respectively

$S(i,j)$ = Segmentation function

$f(i,j)$ = Characteristic feature (gray level) function

T_0, T_1, \dots, T_{m-1} = Threshold values

m = Number of distinct labels to be applied to the image¹¹

If $m = 1$, then thresholding is defined as binary thresholding, and if $m > 1$ then the thresholding is described as multimodal (multilevel) thresholding¹¹.

Binary thresholding makes use of only one threshold value. Every pixel in an image is compared with the threshold chosen. The pixels whose intensity values are below the threshold are set to logical zero (black), the pixels with intensity values above the threshold are set to logical one (white). Hence, this process creates a binary image. The pixels with value 'one' are 'foreground' pixels, and pixels with the value 'zero' are 'background' pixels.

Multilevel thresholding makes use of more than one threshold value. For example, if there are two thresholds $T_1 < T_2$, multilevel thresholding classifies a point (x, y) as belonging to

Intercomparison of image segmentation algorithms one object if $T_1 < I(x, y) \leq T_2$, to the other object class if $I(x, y) > T_2$, and to the background if $I(x, y) \leq T_1$ ⁸, where $I(x, y)$ is the intensity of a pixel at spatial co-ordinates (x, y) .

Figure 4.2.1 is a schematic illustrating the difference between binary thresholding and multilevel thresholding.

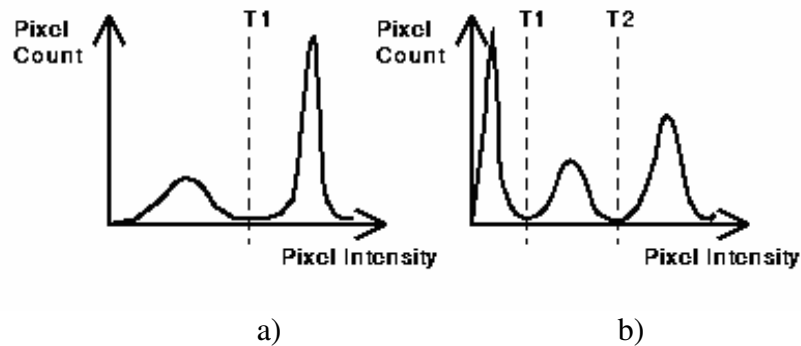


Figure 4.2.1 a) Binary thresholding; b) Multilevel thresholding¹⁶.

According to some properties, a threshold ‘T’ can also be classified into three different categories. If ‘T’ depends only on the gray level value $I(x, y)$ in an image, then it is global thresholding. If ‘T’ depends on both $I(x, y)$ and some local property of pixel $p(x, y)$ then it is called local thresholding. If ‘T’ depends on the spatial co-ordinates (x, y) of an image, then it is dynamic or adaptive thresholding.

Global thresholding makes use of a fixed threshold value to compare all the pixels in an image. However, global thresholding can work well only when the histogram of an image has clear and distinct peaks against its background. Thus, global thresholding fails to give accurate results for images having uneven illumination. For example, shadows can create uneven illumination in an image. In such cases, local or adaptive versions of thresholding yield better results. Adaptive thresholding selects an individual threshold for a pixel based on its intensity ranges. As a result, it provides better results even when the peaks in the

histogram of an image are not distinct, and thus overcomes the problem seen in global thresholding.

In order to find the threshold value in an adaptive thresholding method, two main approaches are used. The first approach is termed the ‘Chow and Kanenko’ approach, and the second is the ‘Local Thresholding’ approach⁴⁶. Both methods use the same assumption; that smaller regions in an image are more suitable for thresholding, as these smaller regions have approximately uniform illumination. In the Chow and Kanenko approach, an input image is divided into an array of sub-images. For every sub-image, an optimum threshold value is computed by examining its corresponding histogram. However, in practice, this method is computationally expensive and therefore its application in real-time problems is difficult. The Local Thresholding approach, on the other hand, uses a statistical method. The mean and the median value for an input image are calculated and these values are used to compute the threshold value. Unlike the ‘Chow and Kanenko’ approach, this method is simple and fast to implement.

Image segmentation using thresholding has several advantages and disadvantages. It is fast and simple. On the other hand, thresholding can generate only two classes of image (binary image) and hence finds less application while dealing with multi-channel images. In addition to this, it does not take into account the spatial characteristics of an image. This makes it sensitive to image artefacts like noise and intensity inhomogeneities. These artefacts can affect the histogram of the image, making separation more difficult. However, the thresholding technique is still in use and is usually the first step in the image segmentation process followed by other image segmentation methods.

In this thesis, the thresholding method was achieved by writing a program using Matlab[®]. The results obtained are presented in Chapter 5. Both the global and adaptive thresholding methods were implemented.

4.2.2 Region Growing

The main objective of image segmentation using region-growing techniques is to partition an image into regions. This method exploits the fact that in an image, the pixels, which are closer spatially to each other, usually have the same gray level values. Region growing is a technique used for extracting a region from an image that is connected, based on some pre-defined criteria. These criteria are based on some characteristic of an image, such as intensity information, edges in an image, texture, shape, colour and size.

Mathematically, region growing is defined by the equations below.

Let ' R ' represent the entire region of the image.

Let $R_1, R_2, R_3, \dots, R_n$, represent ' n ' sub-regions that are obtained after segmenting the entire region R , such that,

$$\bigcup_{i=1}^n R_i = R, \quad (4.2.2.1)$$

$$R_i \text{ is a connected region, } i=1,2,3,\dots,n \quad (4.2.2.2)$$

$$R_i \cap R_j = \phi \text{ for all } i \text{ and } j, i \neq j, \quad (4.2.2.3)$$

$$P(R_i) = \text{TRUE, for, } i=1,2,3,\dots,n, \text{ and} \quad (4.2.2.4)$$

$$P(R_i \cup R_j) = \text{FALSE for } i \neq j \quad (4.2.2.5)$$

where, $P(R_i)$ is logical predicate over the points in the set R_i and ϕ is the null set.

Eq.(4.2.2.1) indicates that every pixel should be in the region. Eq.(4.2.2.2) indicates that a region must be connected. Eq.(4.2.2.3) indicates that the region must be disjoint. Eqs. (4.2.2.4) and (4.2.2.5) indicate the properties that must be satisfied by the pixels in a segmented region. For instance, $P(R_i)$ is true if all the pixels in R_i have the same intensity¹¹.

In order to segment an image using the region growing method, a seed point (pixel intensity) is manually selected by an operator. The operator can also choose more than

Intercomparison of image segmentation algorithms one seed. Sometimes it is difficult to choose a seed, when there is no prior knowledge or information regarding an image. In such cases, a histogram of an image is plotted and then the seed is selected. This seed, will extract all the pixels connected to the initial value with the same intensity value.

The region growing method is summarized as follows:

1. Choose the seed (pixel) for each region.
2. Check the neighbouring pixels and add them to the region if they are similar to the seeds.
3. Repeat step two for each of the newly added pixels; stop if no more pixels can be added.

Figure 4.2 illustrates the region growing process.

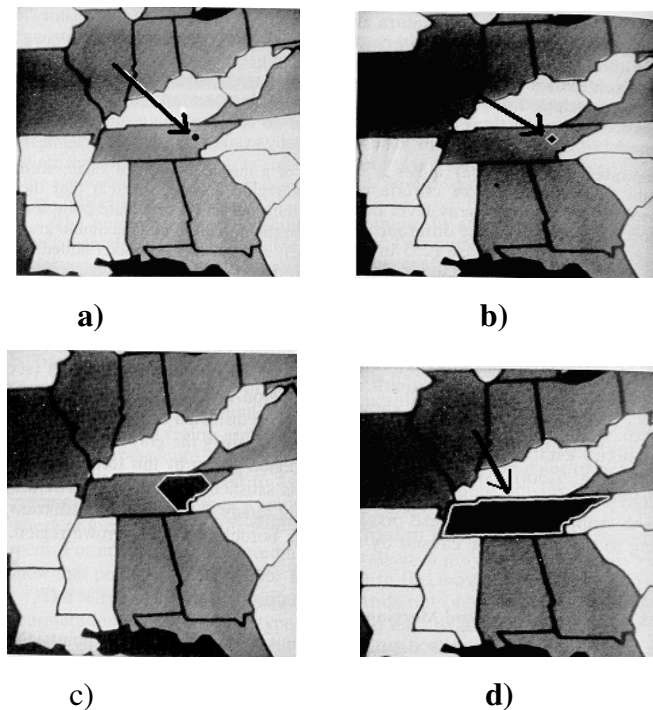


Figure 4.2.2 Segmentation using region growing; a) Original image showing the seed point; b) early stage of region growth; c) intermediate stage of region growth d) final region¹¹.

Region growing has several advantages and disadvantages. One of its main advantages is that it considers the spatial characteristics of an image during segmentation, unlike the thresholding method. The main drawback of the method however, is that it requires manual interaction to obtain a seed point, which is a time-consuming task. In addition to this, the region growing algorithm is also sensitive to noise. As a result, the extracted regions have holes or the regions are disconnected. Conversely, partial volume effects can cause separate regions to be connected¹⁸. In some brain MRI images, the CSF, gray matter and white matter require their own seed for better segmentation. In such cases, precise anatomical information is necessary in order to select the seed, and this process is tedious and time consuming⁴.

Like thresholding, region growing is not often used alone but within a set of image processing algorithms, particularly for the delineation of small, simple structures such as tumours and lesions. Some algorithms, like split and merge algorithms, are used with region growing methods and this provides better image segmentation results.

In this thesis, image segmentation using the region growing algorithm is demonstrated. In order to achieve this, a program is written using Matlab[®], This algorithm is then applied to the simulated images (Section 2.5 describes the simulated image in detail) which is used as a database to obtain the results. The results are presented in Chapter 5.

4.2.3 Edge Based Segmentation

Edge based segmentation algorithms rely on edge detection operators, such as the Laplacian of a Gaussian or Prewitt or Sobel¹⁹. A perfect segmentation could be achieved if we could extract all the edges of an image with the help of additional algorithms such as labeling. However, this is a very difficult task and can rarely be achieved. Most times, the edges that enclose an object are not perfectly detected. Hence, edge based segmentation algorithms are normally followed by supplementary methods which try to join the edges to form edge chains, that is, the boundary that completely encloses the object. A very sophisticated technique based on active contours has been developed, illustrating that this is not an easy task²⁰.

Edge based segmentation is not suitable as a stand-alone technique for medical image segmentation, as it greatly depends on other methods to avoid the disadvantages of edge detection itself. However, some advanced algorithms, like those noted above, provide quite good results when applied to medical images.

4.2.4 Morphological Operators- Watershed Transformation Algorithms

In general, the term ‘morphology’ refers to the study of shapes and structures of an object using mathematical set theory. In the field of image processing, morphology involves analysing the structures and shapes that exist in an image. The morphological operators help in simplifying an image for further analysis and help remove irrelevancies. Morphological operators are used in a number of applications like edge detection and segmentation. These morphological operators transform the original image into another image, achieved by using morphological operators like structuring element. The structuring element is selected based on the shape of the image. For example, for brain MRI images, a ‘disk’ shaped structuring element is chosen. Geometric features that are similar to the structuring element will be preserved in the original image, while other features are suppressed. In addition to structuring elements, there are various other morphological operators like erosion and dilation. Chapter 3 describes these morphological operators in detail. In this section, watershed concepts and watershed transformation algorithms are discussed in detail.

Watershed Concept

The watershed transform is based on morphological operators. H. Digabel and C. Lantuéjoul, first introduced the concept of watershed transformations as a morphological tool³⁵. A few years later, C. Lantuéjoul and S. Beucher³⁹ carried out advanced work that led to the ‘inversion’ of this original algorithm in order to extend it to the more general framework of grayscale images. Later, many other researchers have studied the watershed concept and used it in numerous grayscale segmentation problems¹².

Intercomparison of image segmentation algorithms

The concept of watershed was first used in the field of topography. The watershed concept can be explained by the behavior of water in a landscape. Drops of rainwater fall in different regions and then follow the landscape downhill. These water drops are finally collected at the bottom of a valley. Each valley is associated with a catchment basin, which is unique to every point in the landscape. Watersheds are the divide lines which separate these basins. An alternative approach is to imagine the landscape being immersed in a lake, with holes pierced in local minima. Catchment basins will fill up with water starting at these local minima, and at points where water coming from different basins meet, dams are built. When the water level has reached the highest peak in the landscape, the process is terminated. As a result, the landscape is partitioned into regions or basins separated by dams, called watershed lines or simply watersheds.

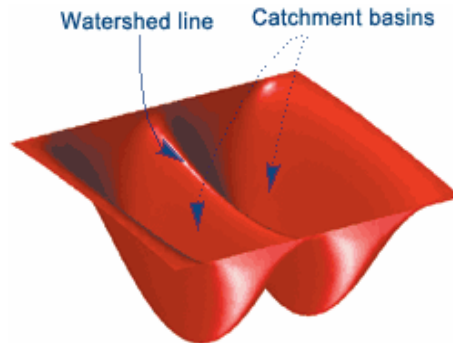


Figure 4.2.4.1 Watershed concept. The figure shows the watershed line and the catchment basin³⁸.

Image Segmentation using Watershed Algorithms

In the field of image processing, and more particularly in mathematical morphology, grayscale images are often considered as topographic reliefs. In the topographic representation of a given image, the numerical value (i.e., the gray level) of each pixel stands for the elevation at this point. Such a representation is extremely useful, since it allows better appreciation of the effect of a given transformation on the image⁴⁰.

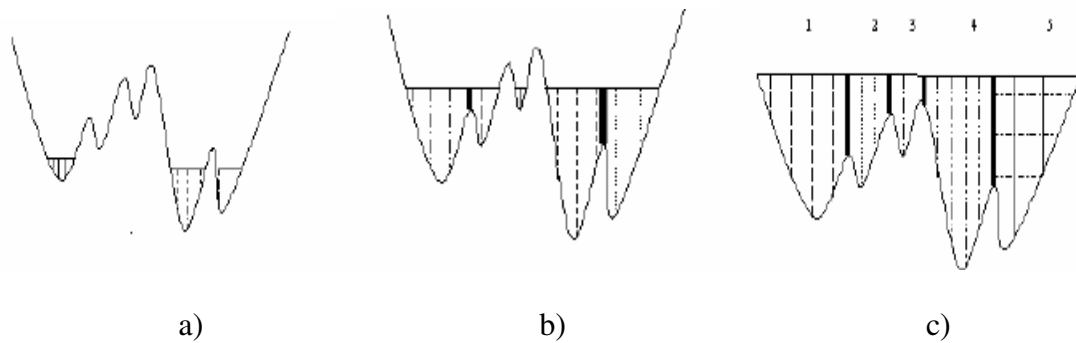


Figure 4.2.4.2 The watershed algorithm. a) shows the flooding from level zero; b) a dam is built where two basins meet; c) shows the conclusion of the process⁴⁰.

In image segmentation, two techniques are followed to segment an image using the watershed algorithm. The first one is the gradient watershed algorithm and the second is the marker controlled watershed algorithm.

The gradient watershed algorithm is used in applications where the edges of an object have to be determined. In this method, the first step is to find the gradient magnitude of an image, then, the watersheds in that region are found. The area in an image where there is a rapid intensity change represents the area of high gradient magnitude. This method usually leads to over-segmentation^{37, 45}.

Meyer and Beucher proposed the marker-controlled watershed algorithm³⁷. In this method, the markers are chosen that are used to mark the objects in an image. These are called ‘object markers’. Similarly, background markers are also chosen. Then the segmentation function is modified such that it has only the minima, foreground markers and background markers. This can be done by modifying the gradient magnitude image so that its only regional minima occur at foreground and background marker pixels. Finally, the watershed transform is performed on the modified segmented function. This method overcomes the over-segmentation problem

Some methods have been developed to make the watershed transform a more robust tool for medical image segmentation¹³. An improvement is presented that allows the

Intercomparison of image segmentation algorithms introduction of prior information for the segmentation process, obtaining satisfactory results. However, the complexity of the algorithm is significant and the use of markers to guide the segmentation process is required, which is a similar problem to the introduction of seeds in the region-growing algorithm.

4.2.5 Clustering

Clustering is a very useful and robust method for image segmentation. The task of clustering is to group and segment a collection of objects into subsets or clusters, such that those within each cluster are more closely related to one another than the objects assigned to different clusters^{21,22}. A cluster is therefore a collection of objects which are ‘similar’ to each other and are ‘dissimilar’ to the objects belonging to the other clusters. Many different types of clustering have been performed, from thresholding to k-means clustering and fuzzy clustering. Clustering essentially seeks to segment the pixel brightness or density into clusters of similar density. Clustering may be classified into the following four subgroups²³:

1. Classical methods.
2. Statistical methods.
3. Neural network methods.
4. Fuzzy clustering methods.

Comparisons have been made of the different methods, by quoting results from various papers²⁴. It was shown that classical methods, such as thresholding and edge based techniques were the least successful methods of segmenting medical images²⁴.

Statistical methods, such as the maximum-likelihood-classifier (MLC) gave satisfactory results, but were reliant on prior knowledge and subject to error if the initial clusters were not well-positioned.

Neural network methods have proved to be more successful than both statistical and classical methods, but have still had difficulty with the uncertainty inherent in medical images.

The final type of method reviewed is fuzzy clustering. The results compared well with those of neural networks, although certain algorithms took longer to segment than neural networks and were sensitive to noise.

Three commonly-used clustering algorithms are the K-means or ISODATA algorithm, the Fuzzy C Means (FCM) and the Expectation Maximization (EM) algorithm^{25, 26}. Many researches in brain MRI segmentation have employed the FCM algorithm. As in ²⁶, presented a knowledge-based classification and tissue labeling approach to initially segment MR brain images using the FCM algorithm, and introduced an expert system to locate a landmark tissue by matching it with a prior model ²⁷ segmenting brain MR images using an artificial neural network (ANN), and compared the performance with FCM. FCM was shown to be superior on normal brains, but worse on abnormal brains with edema, tumor etc. In the research carried in²⁸ they extended the traditional FCM algorithm to deal with MR images corrupted by intensity inhomogeneities. Unfortunately, the greatest shortcoming of FCM is its over-sensitivity to noise, which is also a flaw in many other intensity-based segmentation methods.

4.2.6 K-Means Clustering

The simplest and most efficient type of segmentation is classical segmentation, where k-means clustering is a good example. The process involves segmenting an image into a given number of clusters, therefore making it a supervised algorithm. Supervised algorithms rely on prior knowledge of the image densities, as the number of clusters must be chosen before the image is segmented. The algorithm picks initial density values for each cluster that the image is to be divided into. It then computes a simple Euclidean distance between each pixel in the image and each cluster centre²⁹.

Each pixel is then assigned to the cluster of which the centre is closest to it. Once this is complete the average density for each cluster is computed and this becomes the new cluster centre. This process is repeated and keeps repeating until the cluster centers do not change. After the process is complete, the image is divided into a number of clusters of

Intercomparison of image segmentation algorithms equal density and is therefore segmented³⁰. Although k-means is an effective clustering technique, it has limited applications to segmenting medical images. The uncertainty in the images makes such hard clustering an inaccurate method of segmenting medical images.

The algorithm can be described as follows²⁹:

1. Place k centroids of the initial groups uniformly in the feature space.
2. Assign each object to the group whose centroid lies most closely to this object.
3. When all objects have been assigned, re-calculate the positions of the k centroids,
4. Repeat steps 2 and 3 until the centroids no longer move.

4.3 Fuzzy C Means Clustering

This clustering analysis is based on partitioning the data into a number of subgroups or clusters. The objects located within each cluster must show a degree of similarity. In hard clustering such as k -means, each point in the data is assigned to only one cluster. With the use of fuzzy clustering, each pixel has some degree of membership to each cluster. The degree of membership is an indication of how similar or close a pixel is to some criterion^{31, 32}.

The fuzzy c-means algorithm can be regarded as a pixel classification scheme. Each pixel is classified and segmented according to its grey value in the image. The advantage of the fuzzy c-means method over other methods of segmentation, such as classical and statistical techniques, is that the algorithm does not require any prior knowledge of the data and it is robust to noisy data.

The fuzzy c-means algorithm³³ is based on minimization of the following objective function, with respect to U , a fuzzy c-partition and V a set of cluster prototypes.

$$J_q(U, V) = \sum_{j=1}^N \sum_{i=1}^K (u_{ij})^2 d^2(\mathbf{x}_j, \mathbf{v}_j) \quad K \leq N \quad (4.3.1)$$

Intercomparison of image segmentation algorithms

In eq. (4.3.1), J is the objective function to be minimized, and U is a fuzzy c -partition of the data set. The value of q is any real number greater than 1 and is a weighting exponent on each fuzzy membership. The weighting exponent q allows us to alter the ‘fuzziness’ of the equation. The higher the value of q , the ‘fuzzier’ the equation becomes. If the value of q is 1 the equation simply becomes the k -means clustering algorithm. \mathbf{x}_j is the j -th m -dimensional feature vector or data point in this case, \mathbf{v}_i is the centroid of the i -th cluster, \mathbf{u}_{ij} is the degree of membership of the data point \mathbf{x}_j in the i -th cluster, $d^2(\mathbf{x}_j, \mathbf{v}_i)$ is any distance measure between the cluster centre \mathbf{v}_i and the data point \mathbf{x}_j , N is the number of data points, and finally K is the number of clusters.

To create a fuzzy partition of the data, iterative optimization of eq.(4.3.1) needs to be carried out. The following steps do this:

1. Choose primary cluster centers \mathbf{v}_i . This can be done randomly, or initial estimates may be chosen by examining the histogram of the image.
2. Compute the degree of membership of each data point to all the clusters. Membership is calculated from eq. (4.3.2) below:

$$\mathbf{u}_{ij} = \frac{\left[\frac{1}{d^2(\mathbf{x}_j, \mathbf{v}_i)} \right]}{\sum_{k=1}^K \left[\frac{1}{d^2(\mathbf{x}_j, \mathbf{v}_k)} \right]^{\frac{1}{(q-1)}}} \quad (4.3.2)$$

3. Compute new cluster centers \mathbf{v}_i according to eq.(4.3.3) below:

$$\mathbf{v}_i = \frac{\sum_{j=1}^N (\mathbf{u}_{ij})^q \mathbf{x}_j}{\sum_{j=1}^N (\mathbf{u}_{ij})^q} \quad (4.3.3)$$

Once the new clusters have been calculated, the degree of fuzzy membership must be updated from u_{ij} to \hat{u}_{ij}

4. Check the termination criterion to determine whether iteration is required. The criterion is given by eq.(4.3.4)

$$\text{If, } \max \left\| \mathbf{u}_{ij} - \hat{\mathbf{u}}_{ij} \right\| < \varepsilon \quad (4.3.4)$$

where ε is a termination criterion between 0 and 1

Once the error criterion is reached, the iterative process is complete and the data is separated in a fuzzy partition. From eq.(4.3.2), when calculating the degree of fuzzy membership, the distance measure $d^2(\mathbf{x}_j, \mathbf{v}_i)$ is used. When the distance measure represents the Euclidean distance, the fuzzy c-means algorithm is the result.

The final result is an image partitioned into a number of clusters, the number chosen by the user before running the algorithm. Each pixel in a cluster has a degree of membership associated with it. This degree of membership is an indication of how closely that pixel is associated with its cluster and is a number between [0,1]. When the number is high, e.g. 0.98, that pixel is strongly associated with its particular cluster, but still leaves a degree of uncertainty. To separate the image into partitions, the algorithm looks at the degree of fuzzy membership to each cluster, and assigns the pixel to the cluster that has the highest degree of membership.

Chapter 5

Results

5.1 Introduction

The main objective of this thesis was to compare the different image segmentation algorithms which were discussed in detail in Chapter 4. In this chapter, results are presented for a few image segmentation algorithms, including the thresholding technique, region growing technique, morphological segmentation using the Watershed algorithm and basic fuzzy c-means algorithm. These algorithms were applied to T1-weighted, T2-weighted and proton density images. An additional work was also carried out, in which an algorithm was developed to demonstrate non-brain region removal in brain MRI images, and was discussed in detail in Chapter 3.

A popular software package, Matlab[®], was employed to develop these algorithms. Matlab[®] Version 6.5 was used. These Matlab[®] source codes are included in the Appendices in this thesis.

The MRI images used for testing algorithms are synthetic and real brain images. The synthetic brain MRI images were obtained from the web-based MRI simulator. This web-based simulator was chosen as an image database in this work. Section 2.5 describes the synthetic images in detail. The algorithms that were developed in this project were applied to simulated brain images that are mentioned in the table 5.1.

1.	T1-weighted 1mm slice thickness, 0% noise, 0% intensity non-uniformity
2.	T2-weighted 1mm slice thickness, 0% noise, 0% intensity non-uniformity
3.	PD-weighted 1mm slice thickness, 0% noise, 0% intensity non-uniformity
4.	T1 –weighted image with 7% noise, 20% RF non uniformity
5.	T2 –weighted image with 7% noise, 20% RF non uniformity
6.	PD –weighted image with 7% noise, 20% RF non uniformity

Table 5.1 Different types of synthetic brain images which were employed in this thesis to test the segmentation algorithms.

In this chapter, the results are presented in various sections and parts. Sections 5.2 and 5.3 give a brief overview of how the algorithms were coded using Matlab[®] and the main parameters involved in achieving the image pre-processing and image segmentation algorithms. Parts A, B, C, D, E present the results obtained for the non-brain region removal method, thresholding technique, region growing technique, morphological segmentation using the Watershed algorithm, and basic fuzzy C-means algorithm, respectively.

5.2 Results – Non-Brain Region Removal

An image pre-processing stage is an important stage in any image segmentation method. This stage comprises several steps including image standardization, histogram equalization, tissue contrast enhancement and non-brain region removal methods which make use of morphological operators. The image pre-processing technique has already been discussed in detail in Chapter 3.

PART-A presents the results that were obtained after the non-brain region removal in the brain MRI images, using morphological operators. Morphological operators, such as erosion and dilation, were used in order to achieve the non-brain region removal. The structuring element (SE) chosen in the morphological operation is ‘disk’ shaped. The SE chosen for dilation has a higher value than erosion to ensure that the removal is complete.

PART A- Non-Brain Region Removal Using Morphological Operators

Example 1. T1-Weighted Image

The input image Figure 5.2.1a) is the T1-Weighted image with 1mm slice thickness, 0% noise, and 0% intensity non-uniformity.

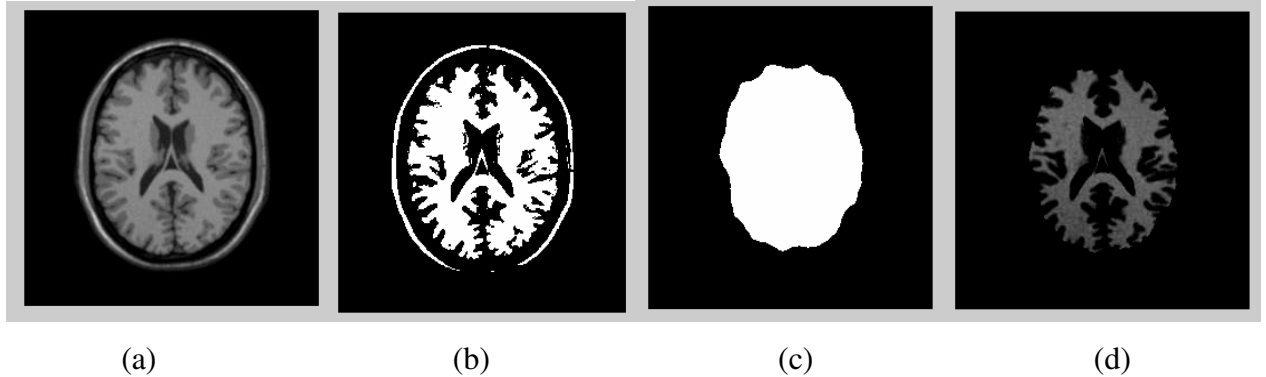


Figure 5.2.1 a) input image; b) binary image obtained after thresholding; c) mask after morphological operation; d) output image with non brain regions removed from input image (that has both brain and non-brain regions).

Example 2. T2-wieghted Image

The input image Figure 5.2.2 a) is the T2-weighted image with 1mm slice thickness, 0% noise, 0% intensity non-uniformity.

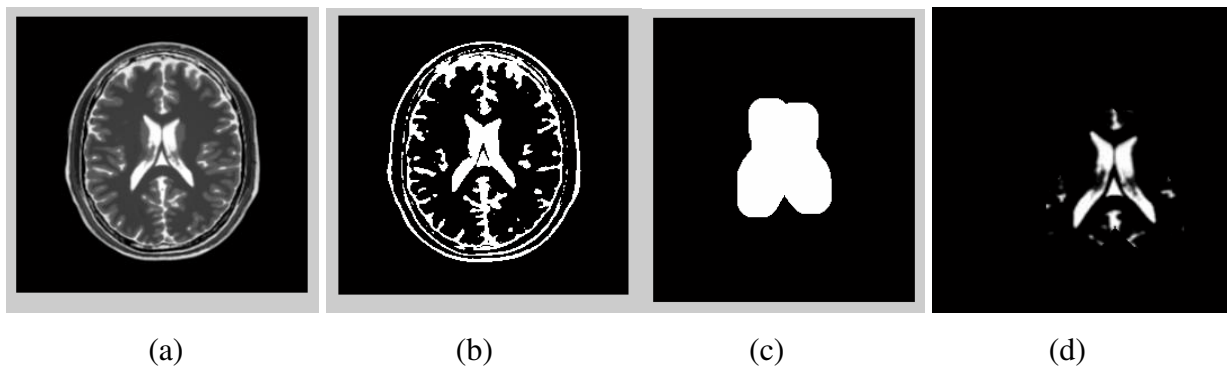


Figure 5.2.2 a) input image; b) binary image obtained after thresholding; c) mask after morphological operation; d) output image with non brain regions removed from input image (that has both brain and non-brain regions).

Example 3. PD-Weighted Image

The input image Figure 5.2.3 a) is the PD image with 1mm slice thickness, 0% noise, and 0% intensity non-uniformity.

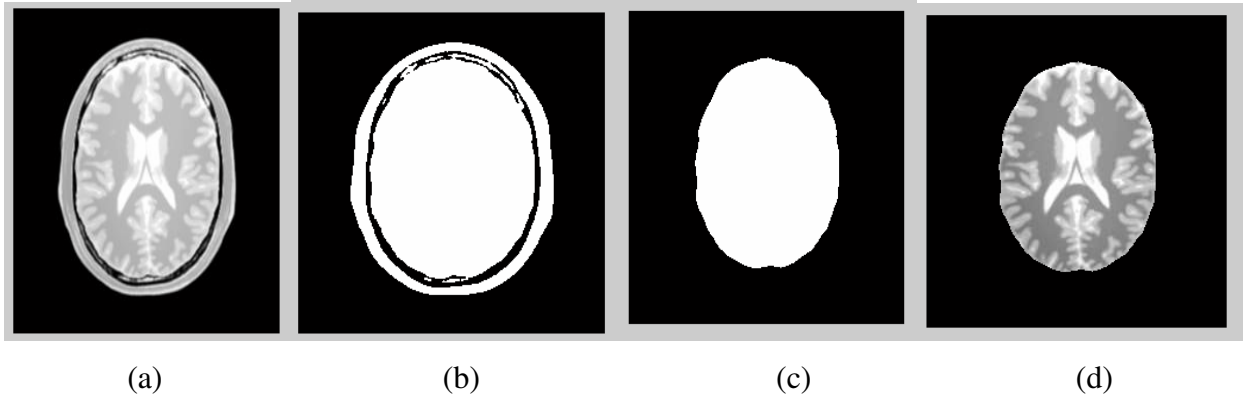


Figure 5.2.3 a) input image; b) binary image obtained after thresholding; c) mask after morphological operation; d) output image with non brain regions removed from input image (that has both brain and non-brain regions).

5.3 Results using Simulated Images - Image Segmentation Algorithms

Image segmentation plays a pivotal role in image processing. There are several algorithms that can be used to segment an image. Some algorithms are used on their own to segment

Intercomparison of image segmentation algorithms an image, while few are used as a combination of different basic algorithms. The most important and the basic segmentation algorithms are the thresholding, region growing technique, segmentation using morphological operators, edge based segmentation and clustering algorithm.

In this section, PART-B presents the results obtained by thresholding method. Thresholding is the oldest and the simplest method employed to segment an image. Both the global and the adaptive threshold methods were applied to the brain MRI images to obtain the results. Section 3.2.1 has described the thresholding method in detail. The adaptive thresholding was achieved by using the statistical approach. The mean and the median value were found, and then the threshold was calculated using the equation,

$$T = (\text{mean} + \text{median}) / 2, \text{ where } T = \text{Threshold.}$$

Part C presents the results obtained by the region-growing method. A pixel (seed) value is chosen and then all the neighbouring pixels are compared with this seed. If the pixels are the same as the seed then add them to the region, else shrink them that is assign the pixels with the value zero. The original and the output image are displayed. In this work, in order to select the value of a pixel, the histogram of the image was examined and then the gray level corresponding to the highest peak was chosen as the seed. Section 4.2.2 has described region growing in detail

Part D presents the results obtained by segmenting an image using the morphological method. The various morphological operators like erosion, dilation and structural element are chosen. In this work, the watershed algorithm is used to obtain the result that is based on mathematical morphology. In this work, the gradient magnitude is calculated using the mathematical equation, $G = \sqrt{(I_x)^2 + (I_y)^2}$, where I_x and I_y are the and G is the gradient magnitude. The marker controlled watershed algorithm is also applied to the images and the results are presented. The structuring element used is the 'disk' shaped element. Section 4.2.3 has described the watershed algorithm in detail.

Part E presents the results obtained by segmenting the images using the basic fuzzy c-means algorithm. To implement this algorithm, the number of clusters is chosen randomly. However, in this work, the algorithm makes use of 4 clusters. These 4 clusters represent the skull, white matter, gray matter, CSF. Chapter 4 has described the basic fuzzy c-means algorithm in detail.

Note that image segmentation algorithms that were developed in this thesis were applied after performing the normalization (standardisation) on MRI images. The normalization was performed based on the concept developed by Shen ⁴. Section 3.1 in this thesis describes image normalization in detail.

PART B IMAGE SEGMENTATION - THRESHOLDING

Example 1 T1-Weighted Image

The input image Figure 5.3.1 a) is the T1-Weighted image with 1mm slice thickness, 0% noise, and 0% intensity non-uniformity.

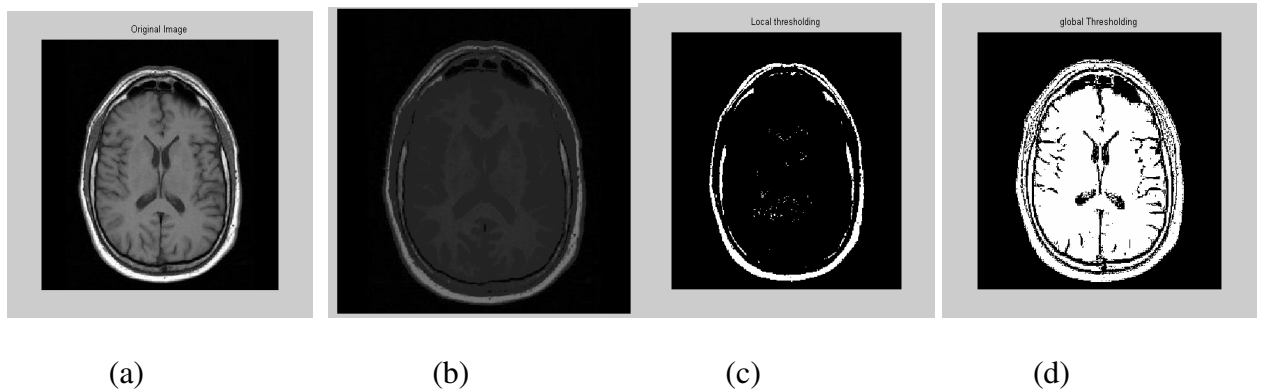


Figure 5.3.1 a) Input image; b) Image is normalised; c) Segmented image using local thresholding method; d) Segmented image using global thresholding method.

Example 2 T2-Weighted Image

The input image figure 5.3.2 a) is the T2-weighted image with 1mm slice thickness, 0% noise, 0% intensity non-uniformity.

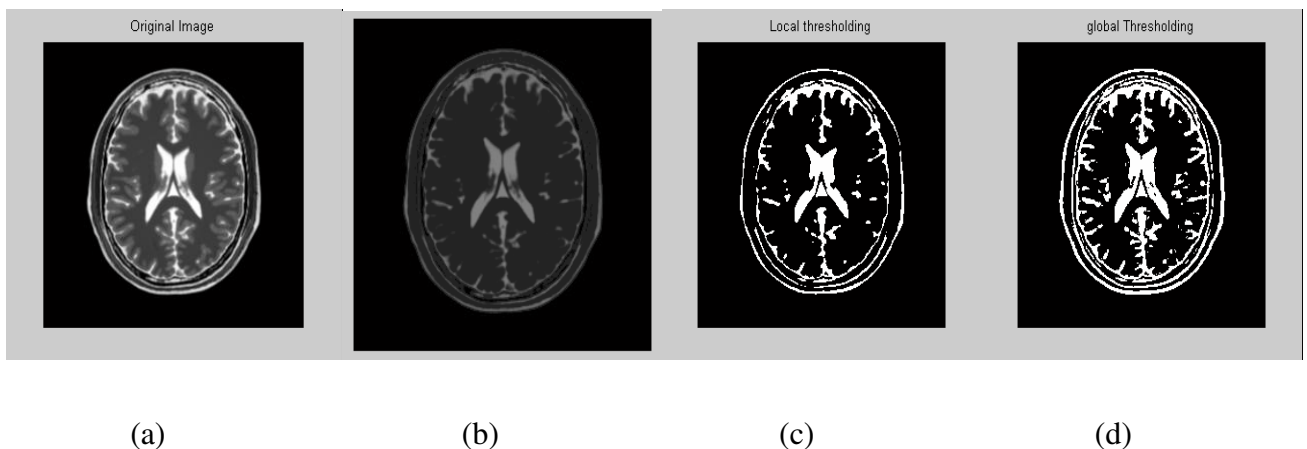


Figure 5.3.2 a) Input image; b) Image is normalised; c) Segmented image using local thresholding method; d) Segmented image using global thresholding method.

Example 3 PD-Weighted Image

The input image Figure 5.3.3 a) is the PD-Weighted image with 1mm slice thickness, 0% noise, and 0% intensity non-uniformity.

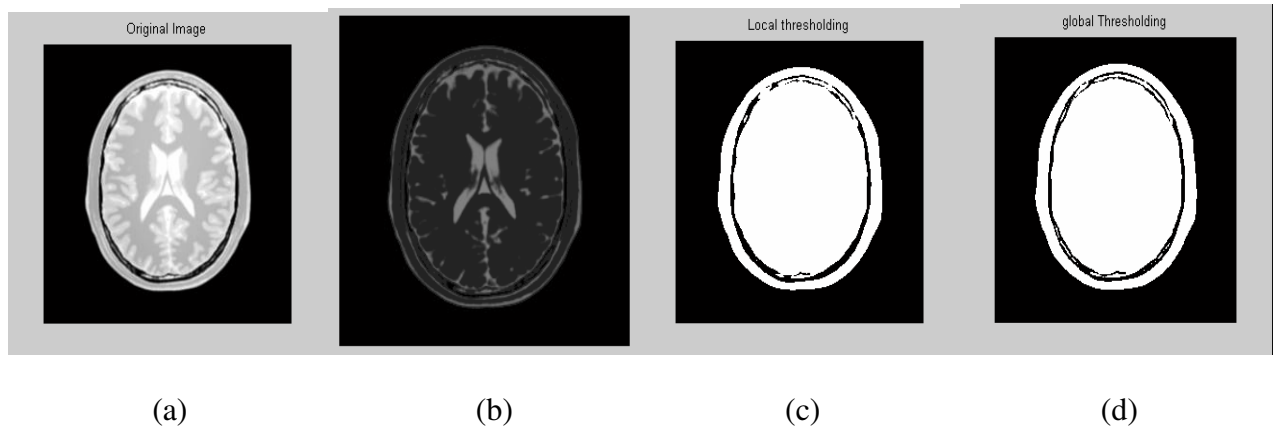


Figure 5.3.3 a) Input image; b) Image is normalised; c) Segmented image using local thresholding method; d) Segmented image using global thresholding method.

PART C IMAGE SEGMENTATION - REGION GROWING

Example 1 T1-Weighted Image

The input image Figure 5.3.4 a) is the T1-weighted image with 1mm slice thickness, 0% noise and 0% intensity non-uniformity.

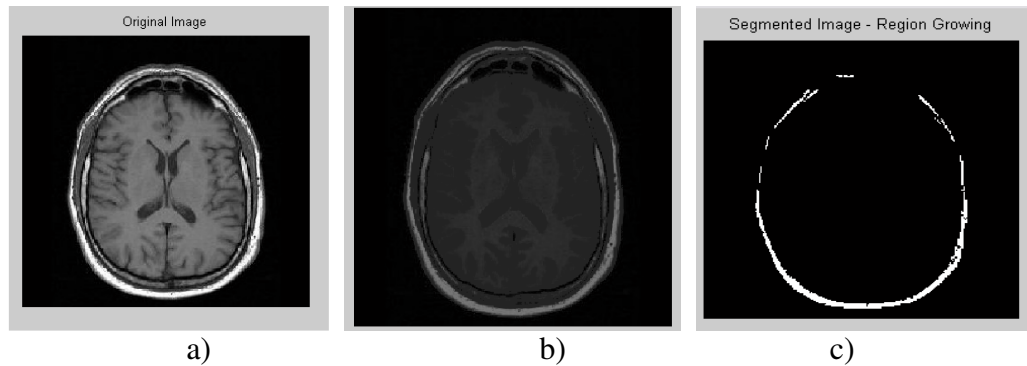


Figure 5.3.4 a) Input image; b) Image is normalized; c) Segmented image using region growing method.

Example 2 T2-Weighted Image

The input image Figure 5.3.5 a) is the T2-weighted image with 1mm slice thickness, 0% noise, and 0% intensity non-uniformity.

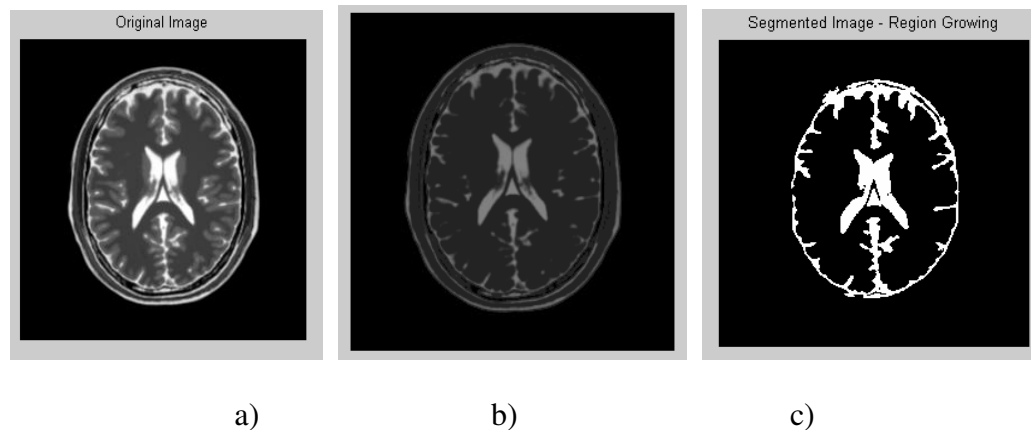


Figure 5.3.5 a) Input image; b) Image is normalized; c) Segmented image using region growing method.

Example 3 PD-Weighted Image

The input image figure 5.3.6 a) is the PD-Weighted image with 1mm slice thickness, 0% noise, and 0% intensity non-uniformity.

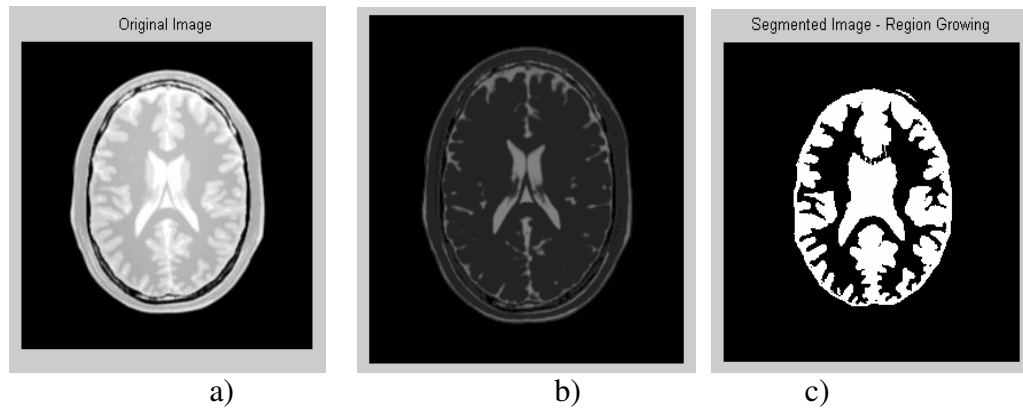


Figure 5.3.6 a) Input image; b) Image is normalized; c) Segmented image using region growing method.

PART D IMAGE SEGMENTATION - WATERSHED ALGORITHM

Example 1 T1-Weighted Image

The input image Figure 5.3.7 a) is the T1-weighted image with 1mm slice thickness, 0% noise, and 0% intensity non-uniformity.

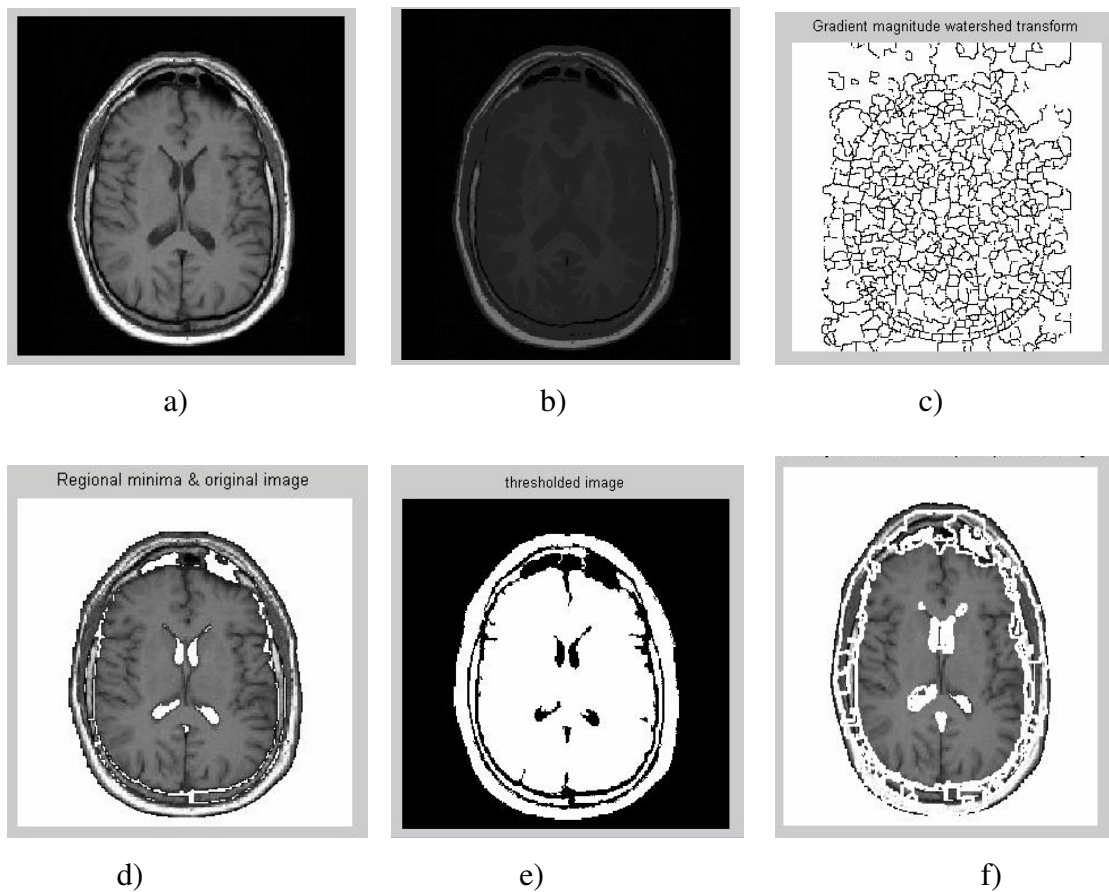


Figure 5.3.7 a) Input image; b) Normalised image; c) Gradient magnitude watershed algorithm (figure shows that this method leads to over-segmentation); d) Regional minima that is for marker controlled watershed algorithm; e) Threshold; f) Markers and object boundaries superimposed in original image.

Example 2 T2-Weighted Image

The input image Figure 5.3.8 a) is the T2-weighted image with 1mm slice thickness, 0% noise, and 0% intensity non-uniformity.

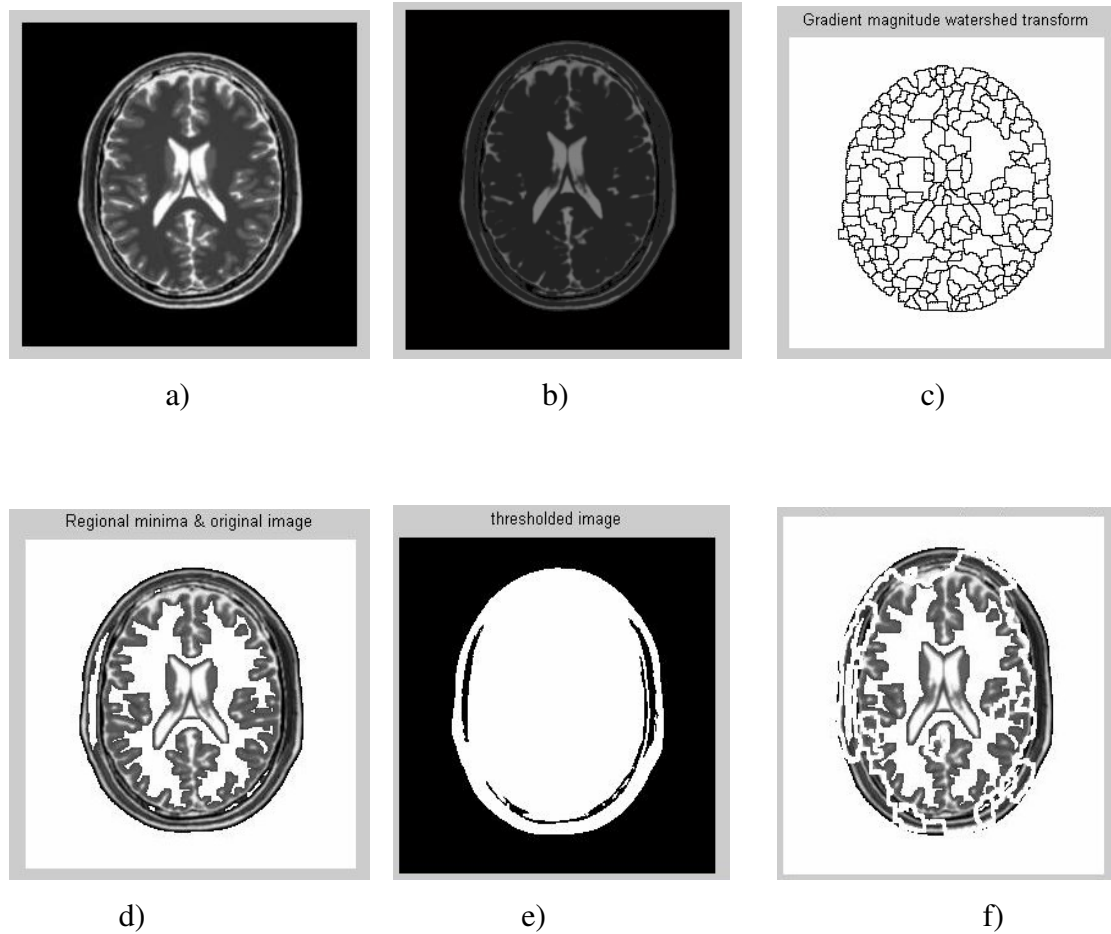


Figure 5.3.8 a) Input image; b) Normalised image; c) Gradient magnitude watershed algorithm (figure shows that this method leads to over-segmentation); d) Regional minima that is for marker controlled watershed algorithm; e) Threshold; f) Markers and object boundaries superimposed in original image.

Example 3 PD-Weighted Image

The input image Figure 5.3.9 a) is the PD-Weighted image with 1mm slice thickness, 0% noise, and 0% intensity non-uniformity.

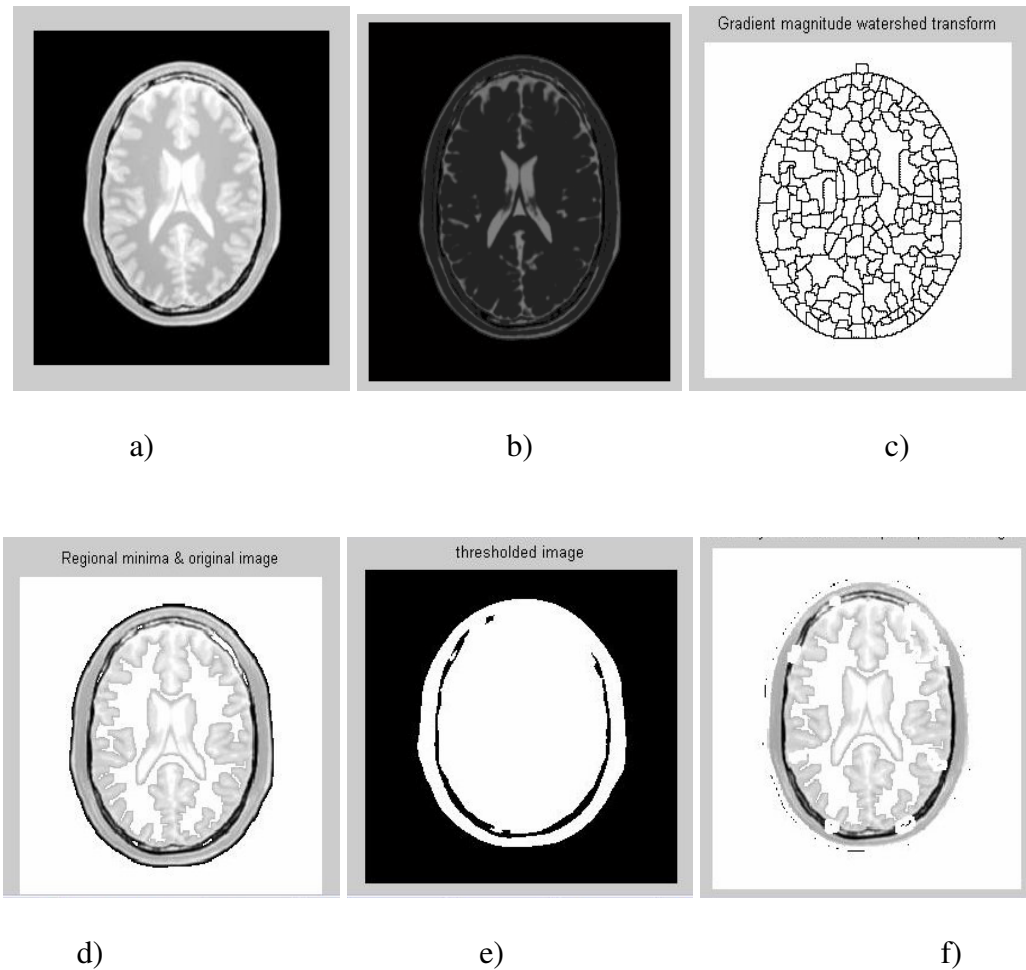


Figure 5.3.9 a) Input image; b) Normalised image; c) Gradient magnitude watershed algorithm (figure shows that this method leads to over-segmentation); d) Regional minima that is for marker controlled watershed algorithm; e) Threshold; f) Markers and object boundaries superimposed in original image.

PART E IMAGE SEGMENTATION – FUZZY C-MEANS**Example1. T1-Weighted Image**

The input image Figure 5.3.10 a) is the T1-weighted image with 1mm slice thickness, 0% noise, and 0% intensity non-uniformity.

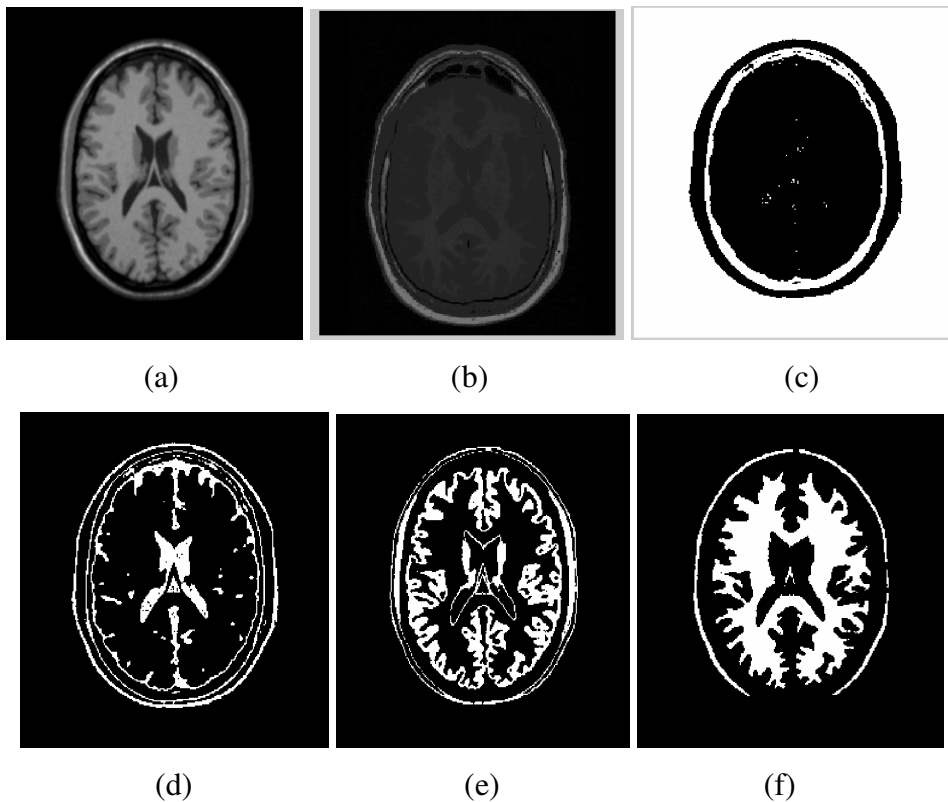


Figure 5.3.10 a) Input image; b) Normalised image that was obtained after performing image standardization c) 1st cluster in the image obtained after segmentation that represents skull; d) 2nd cluster in the image obtained after segmentation that represents CSF; e) 3rd cluster in the image obtained after segmentation that represents white Matter; f) 4th cluster in the image obtained after segmentation that represents Gray Matter.

Example 2. T2-Weighted Image

The input image Figure 5.3.11 a) is the T2-weighted image with 1mm slice thickness, 0% noise, and 0% intensity non-uniformity.

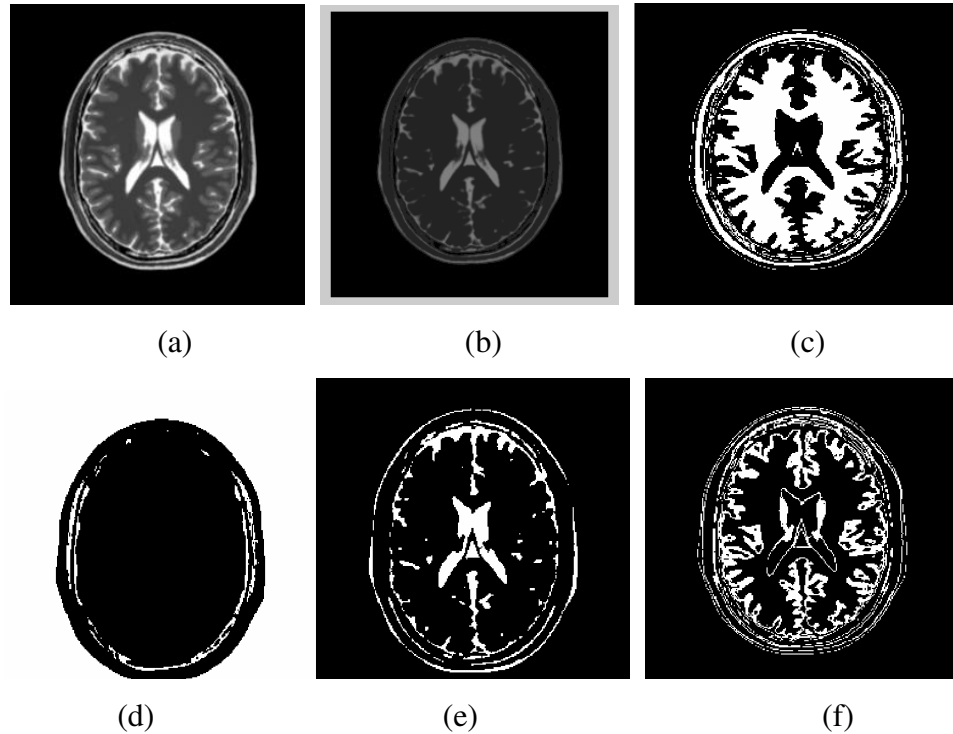


Figure 5.3.11 a) Input image; b) Normalised image that was obtained after performing image standardization c) 1st cluster in the image obtained after segmentation that represents skull; d) 2nd cluster in the image obtained after segmentation that represents CSF; e) 3rd cluster in the image obtained after segmentation that represents white Matter; f) 4th cluster in the image obtained after segmentation that represents Gray Matter.

Example 3. PD Image

The input image Figure 5.3.12 a) is the PD image with 1mm slice thickness, 0% noise, and 0% intensity non-uniformity.

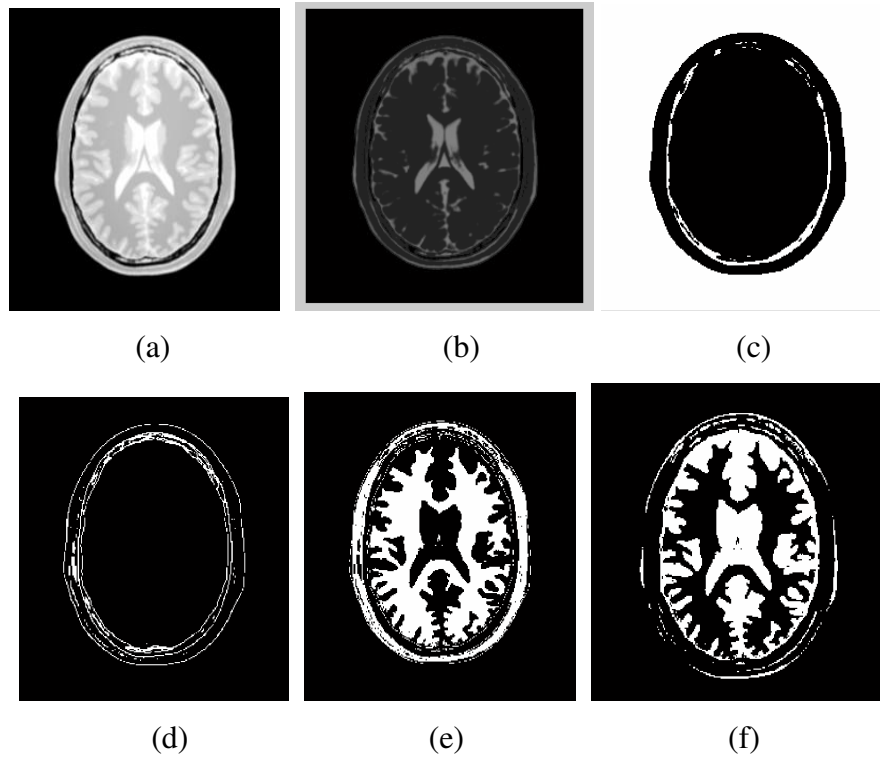


Figure 5.3.12 a) Input image; b) Normalised image that was obtained after performing image standardization c) 1st cluster in the image obtained after segmentation that represents skull; d) 2nd cluster in the image obtained after segmentation that represents CSF; e) 3rd cluster in the image obtained after segmentation that represents white Matter; f) 4th cluster in the image obtained after segmentation that represents Gray Matter.

Example 4. The input image Figure 5.3.13 a) is the T1-weighted image with 1mm slice thickness, 7% noise, and 20% intensity non-uniformity.

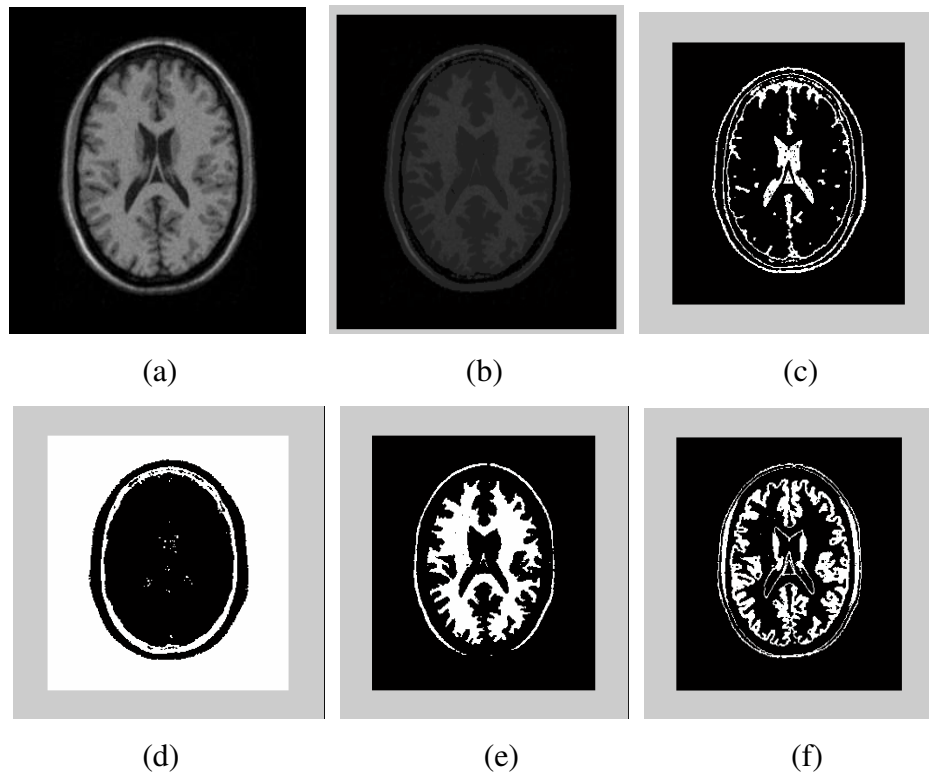


Figure 5.3.13 a) Input image; b) Normalised image that was obtained after performing image standardization c) 1st cluster in the image obtained after segmentation that represents skull; d) 2nd cluster in the image obtained after segmentation that represents CSF; e) 3rd cluster in the image obtained after segmentation that represents white Matter; f) 4th cluster in the image obtained after segmentation that represents Gray Matter.

Example 5. The input image Figure 5.3.14 a) is the T2-Weighted image with 1mm slice thickness, 7% noise, and 20% intensity non-uniformity.

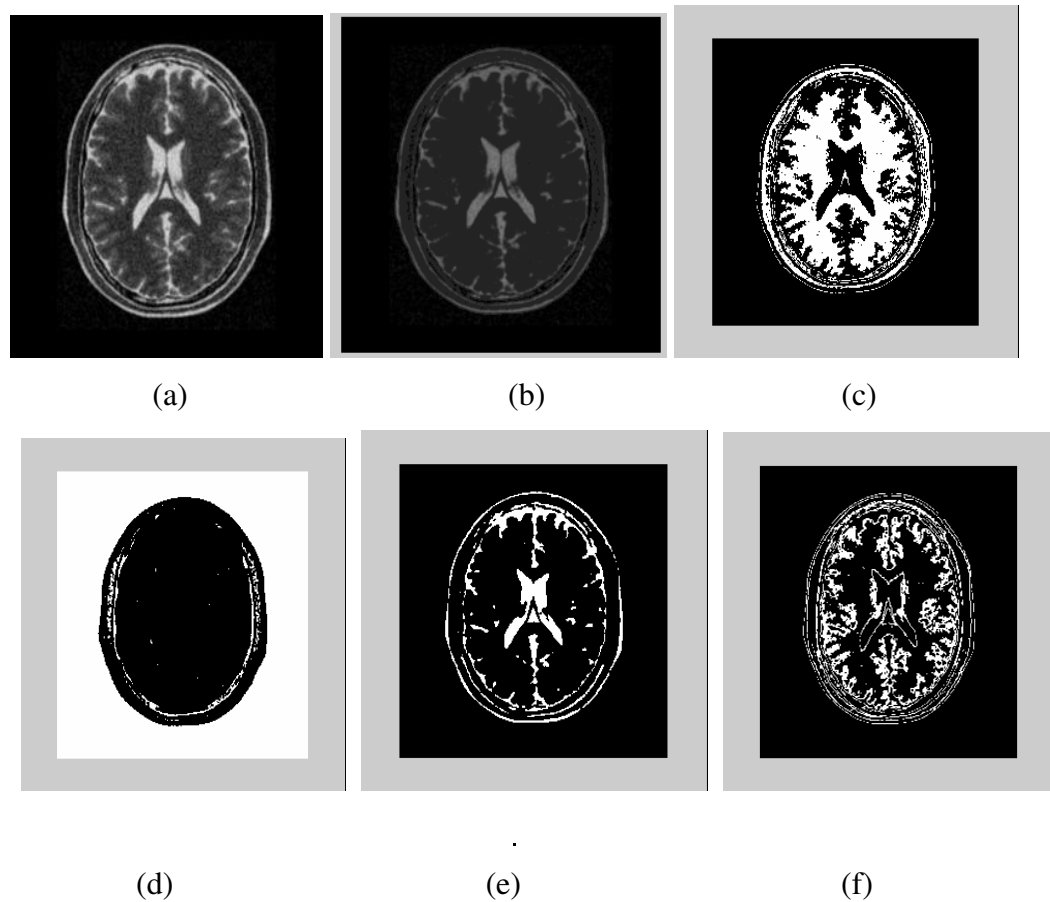


Figure 5.3.14 a) Input image; b) Normalised image that was obtained after performing image standardization c) 1st cluster in the image obtained after segmentation that represents skull; d) 2nd cluster in the image obtained after segmentation that represents CSF; e) 3rd cluster in the image obtained after segmentation that represents white Matter; f) 4th cluster in the image obtained after segmentation that represents Gray Matter.

5.4 Results Using Real Images- Image Segmentation Algorithms

The image segmentation algorithms were applied to a real brain MRI image. This image was obtained from an actual examination recorded on a 1.5 Tesla, GE (Milwaukee, WI) Sigma magnetic resonance imager⁴⁴.

Parts F, G, H, and I in this section represents the results obtained for thresholding, region growing, morphological segmentation and fuzzy-c-means algorithms, respectively.

PART F IMAGE SEGMENTATION - THRESHOLDING

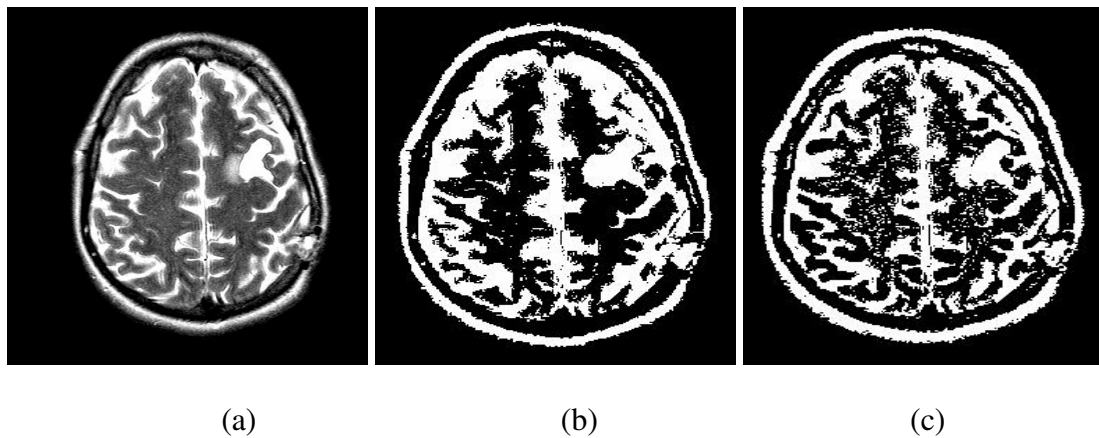


Figure 5.4.1 1 a) Input image; b) Segmented image using local thresholding method; c) Segmented image using global thresholding method.

PART G- IMAGE SEGMENTATION- REGION GRWOING

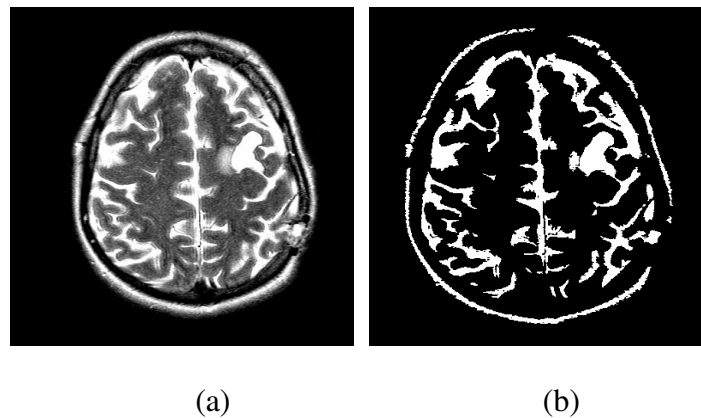


Figure 5.4.2 a) Input image; b) Segmented image using region growing.

PART H- IMAGE SEGMENTATION- WATERSHED ALGORITHM

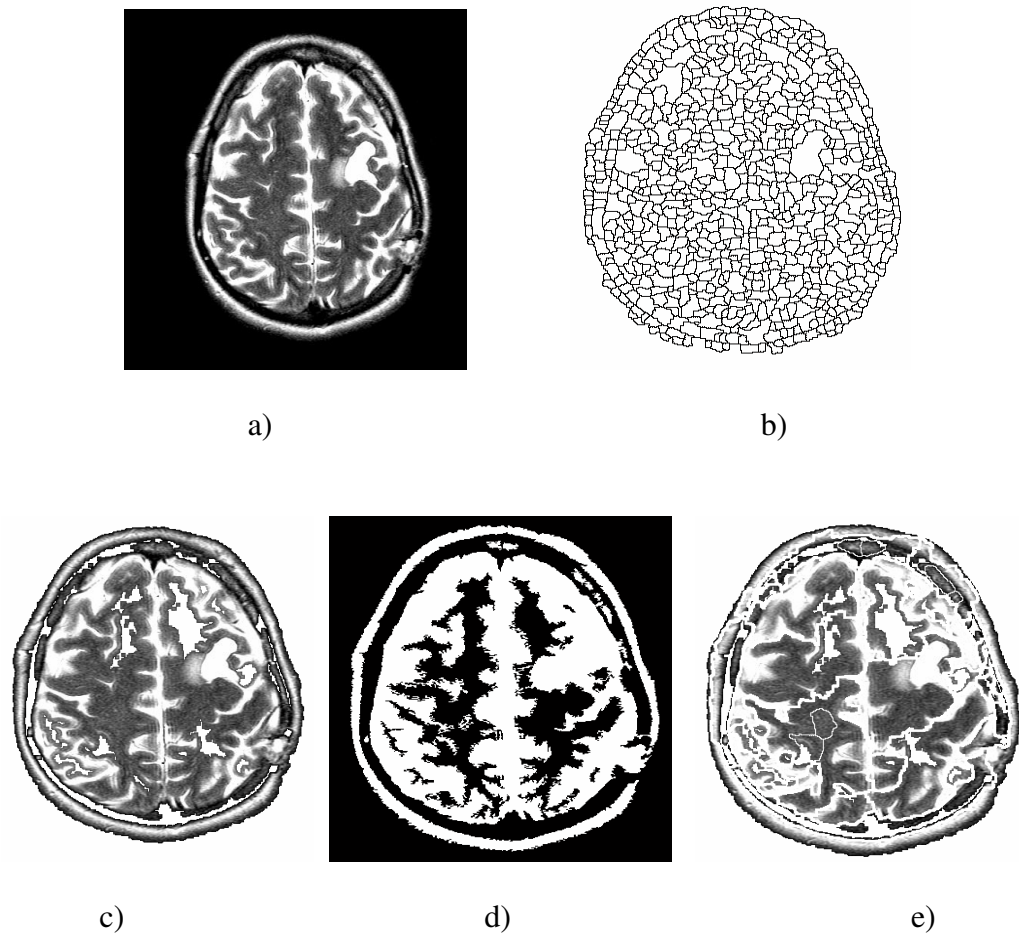


Figure 5.4.3 a) Binary image; b) Gradient magnitude watershed algorithm (figure shows that this method leads to over-segmentation); c) Regional minima that is for marker controlled watershed algorithm; d) Threshold; e) Markers and object boundaries superimposed in original image.

PART I IMAGE SEGMENTATION – FUZZY C-MEANS

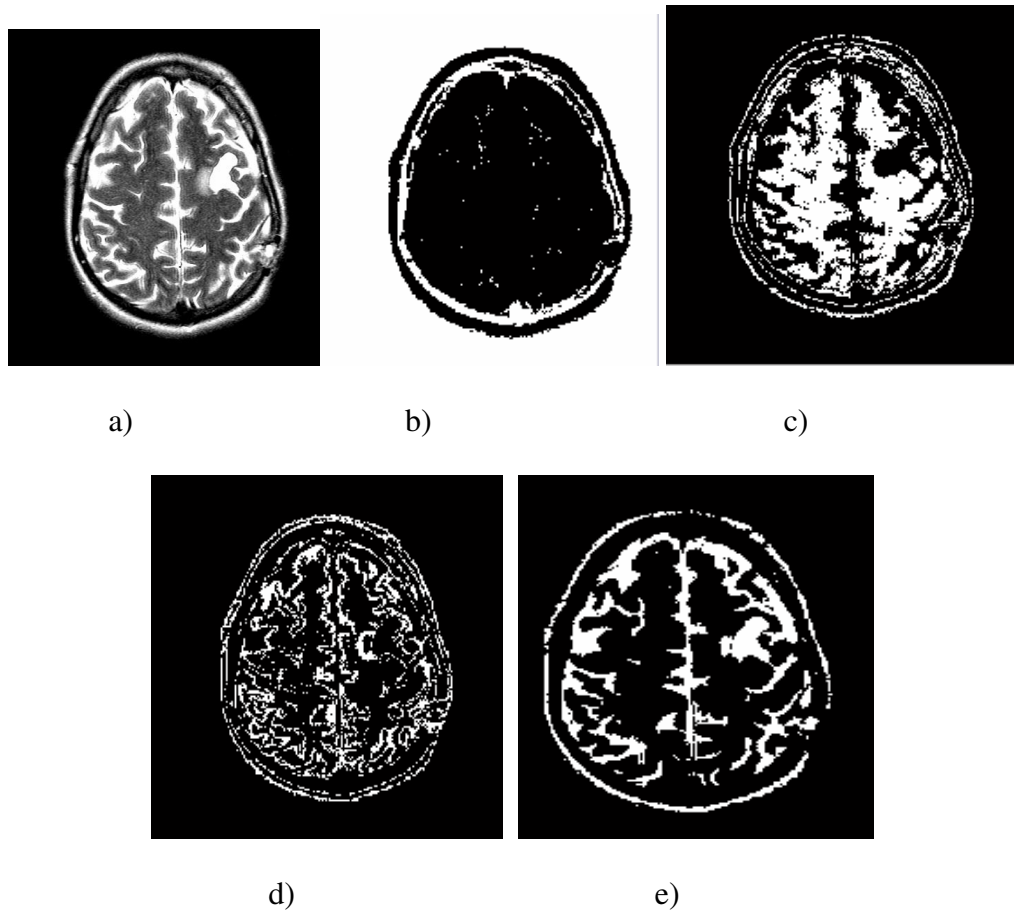


Figure 5.4.4 a) Input image; b) 1st cluster in the image obtained after segmentation that represents skull; c) 2nd cluster in the image obtained after segmentation that represents CSF; d) 3rd cluster in the image obtained after segmentation that represents white Matter; e) 4th cluster in the image obtained after segmentation that represents Gray Matter.

5.5 Comparison of Image Segmentation Algorithms

Image segmentation algorithms are compared both qualitatively and quantitatively. Sections 5.5.1 and 5.5.2 represent qualitative and quantitative comparisons, respectively. The purpose of comparison for different algorithms was to rank their performance and help choosing suitable algorithms according to the application.

5.5.1 A Qualitative Comparison of Image Segmentation Algorithms

A qualitative comparison of algorithms is done visually. Results of thresholding, region growing, morphological method and the fuzzy-c-means algorithm are compared. Algorithms are compared against certain parameters like manual interaction, ability to segment, computational method and a priori knowledge. A brief description as how this comparison was done is mentioned below.

Computational method- Computational method for FCM and watershed algorithm is complex as compared to thresholding and region growing. This is because the FCM and watershed algorithm involve complex equations (For example, the membership equation in FCM. Refer section 4.3 in this for FCM) and hence developing these two algorithms in Matlab program is complex and lengthy as compared to thresholding and region growing.

Priori Knowledge- Thresholding and region growing require a priori knowledge and manual interaction for selecting the pixel intensity (that is, a selection of 'threshold' value for thresholding algorithm and selection of 'seed' for region growing algorithm). FCM and watershed algorithm do not require any priori knowledge and manual interaction.

Ability to segment regions- FCM algorithm could segment the image into different clusters namely CSF, gray matter, white matter and skull. The segmentation of an image using FCM algorithm was more precise than any other algorithms.

The table 5.5.1 shows the comparison between these four algorithms.

	Thresholding	Region growing	Watershed	Fuzzy-C-Means
A-Priori Knowledge	Required	Required	Not required	Not required
Manual Interaction	Required	Required	Not required	Not required
Computational Method	Simple	Simple	Complex	Complex
Ability to segment regions	Average- can segment an image into binary image	Average	Good –marker controlled segmentation provide better segmentation	Excellent
Noise	Sensitive	Sensitive	Very Sensitive- can lead to over segmentation	Sensitive
Spatial characteristics of an image	Not considered	Considered	Considered	Considered

Table 5.5.1 Qualitative comparison of image segmentation algorithms.

It can be noted that each segmentation technique suffers from a few drawbacks. Some algorithms are sensitive to noise, while some require manual interaction. Most algorithms consider only the intensity characteristics of an image. By combining one or two basic algorithms, a more effective algorithm can be developed which aids better image segmentation. Also, to obtain better results the algorithm should not only consider the intensity characteristics of an image but also spatial characteristics of an image.

5.5.2 A Quantitative Comparison of Image Segmentation Algorithms

Quantitative comparison between four segmentation algorithms was performed using simulated images. For carrying out quantitative comparison, two parameters were chosen.

Intercomparison of image segmentation algorithms

Correct segmentation: Number of pixels, which are segmented correctly in the particular region.

Incorrect segmentation: Number of pixels, which are segmented incorrectly in the particular region.

Using the above two parameters, total number of correctly and incorrectly segmented pixels were calculated and were expressed in terms of percentage. The results obtained for quantitative comparisons are displayed in Table 5.5.2.

A program was developed in Matlab[®] to achieve quantitative comparison.

IMAGES WITHOUT NOISE AND ARTEFACTS				
	Thresholding	Region Growing	Morphological Segmentation	Fuzzy-C-Means
Correct Segmentation (%)	89.7	38.2	79.6	91.1
Incorrect Segmentation (%)	9.2	61.6	20.1	8.7
IMAGES WITH NOISE AND ARTEFACTS				
Correct Segmentation (%)	87.1	36.9	77.5	90.7
Incorrect Segmentation (%)	12.2	63.0	22.3	9.2

Table 5.5.2 Quantitative comparison of image segmentation algorithms.

Chapter 6

Conclusions and Future Work

The focus of this project was on image segmentation using brain MRI images. As this thesis incorporates brain MRI images for developing and testing image segmentation algorithms, it is very important to know the basic principles of MRI. An overview of MRI and different parameters involved in MRI were discussed. Also, artefacts including noise, partial volume effects and intensity inhomogeneities were discussed.

In order to test algorithms (algorithms written for image segmentation and non-brain removal) in this thesis an image source or database of brain MRI images was required. These data can be obtained either from internet\website (simulated or synthetic data) or can be collected from hospitals (real data). Different types of MRI brain images with various parameters and databases employed to obtain these images were introduced.

Image pre-processing is a significant stage in image processing. Before performing image segmentation, image pre-processing must be carried out. This helps in achieving better and more accurate image segmentation results. Since the focus of this work was mainly on image segmentation, the image pre-processing method was discussed only briefly. Three main stages of image pre-processing methods - image standardization, non-brain region removal and contrast enhancement were discussed.

Unlike other imaging modalities like CT or x-rays, images obtained from the same MRI machine lack a standard and quantifiable interpretation of image intensities. It is noticed that images obtained from the same MRI scanner may vary for the same person, and same body region at different times. The reason for such variation in MRI images is due to a number of scanner-dependent variations. Hence, displaying and quantitative analysis of such non-standardized images becomes difficult. Therefore image standardization is

Intercomparison of image segmentation algorithms essential. Different methods by which image standardization can be obtained were discussed.

Non-brain region removal is the second step in image pre-processing. The brain MRI includes the whole head image. However, while performing image segmentation, the area of interest is only the brain region. Hence, elimination of non-brain regions is essential to achieve better image segmentation results. The use of morphological operators is one of the most widely used methods in non-brain region removal. These morphological operators were discussed in detail. The Morphological operators were also used in image segmentation.

Tissue contrast enhancement is another important step in image preprocessing. The intensities of the gray matter and white matter in brain regions are very similar in most MRI images. Tissue contrast enhancement aids in distinguishing tissues with similar intensities. Tissue contrast enhancement can be obtained by histogram equalization.

Additionally, an algorithm was written using Matlab[®] using morphological processing to obtain non brain region removal. This algorithm was tested on selected simulated images.

Image segmentation was the focus of this work. There are several methods used to perform image segmentation. Some methods are simple while some are complex. Image segmentation algorithms are mainly divided into three classes - thresholding or clustering, edge based segmentation, and fuzzy method. In this thesis, different image segmentation methods like thresholding, region growing, edge based segmentation, morphological operation, k-means clustering and fuzzy-c-means were discussed in detail. Few of these algorithms were developed using the popular Matlab[®] tool and results were obtained on different MRI images such as T1-weighted, T2-weighted and PD images. A qualitative and quantitative comparison was performed on these algorithms. The purpose of comparison for different algorithms was to rank their performance and help choosing suitable algorithms according to the application. Several parameters were used to achieve qualitative comparison like noise, manual interaction and computational time.

It was observed that these algorithms suffered from a few drawbacks. Some algorithms considered only the intensity characteristics of an image, while some required manual interaction and priori knowledge of an image. Also, most of algorithms were sensitive to noise. The thresholding gave better segmentation results as compared to watershed and region growing algorithm. However, thresholding produces only a binary image. Hence, this algorithm fails to give detail information about a segmented image. Region growing considers requires manual interaction and priori knowledge of an image. Watershed algorithm is very sensitive to noise and leads to over-segmentation. Fuzzy-c-means provided better segmentation results compared to other algorithms both quantitatively and qualitatively. It was less sensitive to noise compared to other algorithms. Overall, it can be concluded that, by combining one or two basic image segmentation algorithms a more effective algorithm can be developed to achieve better image segmentation.

Unfortunately, there was no concrete and reliable information available on World Wide Web regarding which image analysis or segmentation techniques are being used in state of the art commercial (medical) MRI scanners. However, during the work of this thesis, whatever (recent) peer reviewed journals and research papers were studied based on that knowledge it will be fair to suggest that, for (brain) MRI image segmentation Fuzzy based clustering is the widely used and researched segmentation technique. And to improve the segmentation performance of fuzzy based clustering approach, genetic algorithm and neural network techniques are also being used.

This project has accomplished its goals but in the process has uncovered some areas of image segmentation which need to be explored. First of all, future work would involve developing an effective algorithm that is computationally fast and more robust to noise. This can be achieved by considering the strong points of several algorithms. In addition to this, pre-processing methods must be employed before performing image segmentation on brain images, to achieve more accurate results. Secondly, though quantitative comparison was performed on simulated images in this work it did not involve much statistical methods due to time constraint. Hence another scope for future work will include

Intercomparison of image segmentation algorithms performing quantitative comparison using statistical methods that will give better results which in turn will help comparing algorithms in a better way. Thirdly, algorithms were implemented only on one or two real images as acquiring these real images needs significant amount of time due to ethical reasons. Validation of algorithms on further real images is very important as the true application of these algorithm lies on real MR images that are obtained by diagnosing living tissues.

References

1. Faulkner W 1996. 'Basic principles of MRI'.
URL: http://www.e-radiography.net/mriect/Basic_MR.pdf
2. Mackiewicz B 1995. 'MR imaging and data characteristics'.
URL: <http://www.cs.sfu.ca/~stella/papers/blairthesis/main/node9.html>
3. Margaret M 1999. 'Basic principles of MRI'.
URL: <http://www.erads.com/mrimod.htm>
4. Shan S 2004. 'MRI brain tumour classification using image processing and data mining',
Phd thesis in Bioengineering, University of Strathclyde.
5. Ballinger J 1996. Introduction to MRI.URL: <http://www.mritutor.org/mritutor/index.html>
6. Nowak R, 'Wavelet based Rician Noise Removal for the Magnetix Resonance Imaging'.
IEEE Transactions on Image Processing. 1999; vol. 8, no. 10, pp. 654- 689.
7. Neelin P 2001. 'McConnell Brain Imaging Centre, BrainWeb Simulated brain database'.
URL: <http://www.bic.mni.mcgill.ca/brainweb/>
8. Nyul L, Udupa J, 1999. 'On standardizing the MR image intensity scales, Magnetic
Resonance Imaging', vol.42, pp. 1072-1081
9. Siegel A, Morgan C, 'Statistics and Data Analysis- An Introduction'. 2nd ed., John Wiley &
Sons, 1996.
10. Everitt.B, 1989. 'Statistical methods for medical investigations'. Oxford University Press,
USA.
11. Rafael C, Richard E, 'Digital Imaging Processing'. 2nd ed., Upper Saddle River, N.J.Prentice
Hall 2002.
12. Hyun G, 'Morphological Image Segmentation for Co-aligned Multiple Images using
Watersheds Transformation'. The Florida State University College of Engineering, USA.
13. Grau V, Mewes A, Alcañiz M, Kikinis R, Warfield S, 'Improved Watershed Transform for
the Medical Image Segmentation Using Prior Information'. IEEE Transactions on Medical
Imaging. 2004; vol 23, no.4, pp. 970-1022.
14. Desco M, Gispert J, Reig S, Santos A, Pascau J, Malpica N, García P, Barreno,
'Statistical Segmentation of Multidimensional brain datasets'. Hospital General
Universitario Gregorio Marañón, Universidad Politécnica de Madrid.
15. Lynn M, Fletcher H, Hall L, Goldgof D, Murtag F, 'Automated Segmentation of
Non Enhancing Brain Tumours in Magnetic Resonance Images'. Department of
Radiology of the University of South Florida, Tampa, USA.

Intercomparison of image segmentation algorithms

16. Johnston B January 1994. 'Three dimensional multispectral stochastic image segmentation'. MSc thesis in Computer science, University of British Columbia.
17. Jiang M 2000. 'Digital Image Processing'.
URL: <http://iria.math.pku.edu.cn/~jiangm/courses/dip/html/node119.html>
18. Dzung L, Phamé, Jerry L, Princeé 1998. 'A Survey of Current Methods in Medical Image Segmentation'. Department of Electrical and Computer Engineering, The Johns Hopkins University Charles St. Baltimore.
19. Rafael C, Richard E, 'Digital Imaging Processing'. 2nd ed., Upper Saddle River, N.J. Prentice Hall 2002
20. Warren H November 2004. 'Pattern Recognition in the detection of tuberculosis meningitis'. MSc thesis in Biomedical Engineering. University of Capetown.
21. Jhinfeng H 2005. 'Fuzzy C-Means Algorithm for the classification of MRI Images'.
22. Rajapakse J, Giedd J, Rapoport J, 'Statistical Approach to Segmentation of Single-Channel Cerebral MR'. IEEE Transactions on Medical Imaging, 1999; vol.16, no.2, pp. 308-323.
23. Nevin, Mohamed A, Ahmed M, Farag, 'A Modified Fuzzy C-Mean in Medical Image Segmentation'. IEEE Proceedings of the International Conference on Acoustics, Speech and Signal Processing. March 1999; Phoenix, USA.
24. Wells W, Grimson W, Kikinis R, Jolesz F, 'Adaptive Segmentation of MRI Data'. IEEE Transactions on Medical Imaging 1999; vol.15, no.4, pp.429-442.
25. Li C, Goldgof D, Hall O, 'Knowledge-based classification and tissue labelling of MR images of human brain'. IEEE Transactions on Medical Imaging 1993; vol.12, no.4, pp.740-750.
26. Hall L, Bensaid A, Clarke L, Velthuizen R, Silbiger M, Bezdek J, 'A comparison of neural network and fuzzy clustering techniques in segmenting magnetic resonance images of the brain'. IEEE Transaction on Neural Networks 1992; vol.3, no.5, pp.672-682.
27. Pham D, Prince J, 'Adaptive fuzzy segmentation of magnetic resonance images'. IEEE Transactions on Medical Imaging. 1999; vol.18, no.9, pp.737-752.
28. Jhinfeng H 2005. Fuzzy C-Means Algorithm for the classification of MRI Images.
29. Coleman G, Andrews H 1979. 'Image segmentation by clustering'. Proc IEEE; vol 67, no.5, 773-84.
30. Gath I, Geva, 'A Unsupervised Optimal Fuzzy Clustering'. IEEE Transactions on Pattern Analysis and Machine Intelligence 1989; vol 11, no.7, pp.773-781.
31. Bezdek J, Pal S 1992. 'Fuzzy Models for Pattern Recognition'. IEEE Press, Piscataway New York.
32. Bezdek J 1981. 'Pattern Recognition with Fuzzy Objective Function Algorithms'. Plenum Press, New York.

Intercomparison of image segmentation algorithms

33. Banerjee S, Mukherjee D, Majumdar D 1999. 'Fuzzy C-Means Approach to Tissue Classification in Multimodal Medical Imaging'. Information Sciences; vol 115,no1-4,261-279.
34. B.L. Li, Goldgof D, Hall L, 'Knowledge-based classification and tissue labelling of MR images of human brain'. IEEE Transactions on Medical Imaging 1993; vol.12, no.4, pp.740-750.
35. Digabel H, Lantuéjoul C, 'Iterative algorithms', Proc. 2nd European Symp. on Quantitative Analysis of Microstructures in Material Science, Biology and Medicine, October 1977;Caen, France.
36. Leemput K, Maes F, Vandermeulen F, Suetens P, 'Automated model-based tissue classification of MR images of the brain'. IEEE Transactions on Medical Imaging.1999; vol.18, no.10, pp.897-908.
37. Meyer F, Beucher S 1990. 'Morphological segmentation'. Journal of Visual Communication Image Representation 1: 21-46.
38. Eddins S 2002, 'The watershed transform, Strategies for image segmentation'.
URL: www.mathworks.com
39. Lantuéjoul C, Beucher S, 'Use of watersheds in contour detection'. International workshop on Image Processing Real Time Edge Detection/Estimation, September 1979; Rennes France.
40. Georgi Ignatov, Hristo Nikolov, Doyno Petkov, George Georgiev, 'Morphological and object oriented methods in classification of multispectral data'. 2nd Scientific Conference on Space, Ecology, Nanotechnology, Safety. June 2006;Varna, Bulgaria
41. Disher B, Lenarduzzi, Lewis B, Teeuwen J 2006. University of Windsor, Medical Imaging Physics.
URL: http://web2.uwindsor.ca/courses/physics/high_schools/
42. Bloch F, Hansen W, Packard M 1946. 'Nuclear Induction', Physics Rev. ; vol 70,pp 460-473
43. Purcell M, Torrey H, Pound C 1946. 'Resonance Absorption by Nuclear Magnetic Moments in a solid'; Rev. ; vol 69,pp 37-38
44. Honark J 1996. 'Basics of MRI'.
URL: <http://www.cis.rit.edu/htbooks/mri/index.html>
45. Beucher S, 'Image Segmentation and Mathematical Morphology'.
URL: <http://cmm.enscm.fr/~beucher/wshed.html>.
46. Fisher B, Perkins S, Walker A, Wolfart E , 'Hypermedia Image processing reference', Department of Artificial Intelligence, University of Edinburgh, UK

APPENDIX I Glossary

A. Acquisition Matrix: The total number of independent data samples in the frequency and phase directions.

B. Fourier Series Fourier series is a tool used for analyzing an arbitrary function by decomposing it into a weighted sum of much simpler sinusoidal component functions.

C. Gibbs Phenomenon The Gibbs phenomenon also known as the ringing artefacts is the peculiar manner in which the Fourier series of a piecewise continuously differentiable periodic function f , behaves at a jump discontinuity. The n th partial sum of Fourier Series has large oscillations near the jump, which might increase the maximum of the partial sum above that of the function itself. The overshoot does not die out as the frequency increases, but approaches a finite limit. (In mathematics, a function $f(x)$ of a real number variable x is defined piecewise, if it is continuous on all but a finite number of points).

D. Pixel A pixel is a picture element (pictures +elements). Pixels do not have a fixed size. Their diameters are measured in microns. Although the pixel is not a unit of measurement itself, pixels are often used to measure the resolution of the image. For Example, a 600 x 1000 pixel image has 4 times the pixel density and is thus 4 times sharper than a 300 x 500 pixel image, assuming the two images have the same physical size.

E. Undersampling Undersampling is the decrease in the data to increase the image acquisition speed. That is, shorter scans without the loss of quality. For example the quality reduction in the data is normally associated with an increase in the aliasing (the degradation of the signal to noise ratio through backfolding of the entire noise spectrum), or with other artefact caused by missing data, which results in fine lines.

F. Voxel A voxel is a volume element (volumetric and pixel) representing a value in the three dimensional space, corresponding to a pixel for a given slice thickness. Voxels are frequently used in the analysis of the medical data. MRI pixel intensity is proportional to the signal intensity of the appropriate voxel.

APPENDIX II Matlab[®] Functions

A few of the Matlab[®] functions that were used in developing the algorithms are mentioned below.

Matlab[®] functions	Description
<i>imread()</i>	Read image from graphics file.
<i>min()</i>	Smallest component. For vectors, min(X) is the smallest element in X. For matrices, min(X) is a row vector containing the minimum element from each column.
<i>mean()</i>	Average or mean value. For vectors, mean(X) is the mean value of the elements in X. For matrices, mean(X) is a row vector containing the mean value of each column.
<i>max()</i>	Largest component. For vectors, max(X) is the largest element in X. For matrices, max(X) is a row vector containing the maximum element from each column.
<i>abs()</i>	Absolute value. abs(X) is the absolute value of the elements of X. When X is complex, abs(X) is the complex modulus (magnitude) of the elements of X.
<i>im2bw()</i>	Convert image to binary image by thresholding.
<i>strel()</i>	Create morphological structuring element.
<i>imshow()</i>	Display image.
<i>rgb2gray()</i>	Convert RGB image or colormap to grayscale.
<i>imerode()</i>	Erode image. IM2 = imerode(IM,SE) erodes the grayscale, binary, or packed binary image IM, returning the eroded image, IM2. SE is a structuring element object, or array of structuring element objects, returned by the STREL function.
<i>imdilate()</i>	Dilate image. IM2 = imdilate (IM, SE) dilates the grayscale, binary, or packed binary image IM, returning the dilated image, IM2. SE is a structuring element object, or array of structuring element objects, returned by the STREL function.

Intercomparison of image segmentation algorithms

<i>imclose()</i>	Close image.
<i>zeros()</i>	Zeros array. zeros(N) is an N-by-N matrix of zeros.
<i>graythresh()</i>	Compute global image threshold using Otsu's method.
<i>imtophat()</i>	Perform top hat filtering. IM2 = imtophat(IM,SE) performs morphological top hat filtering on the grayscale or binary input image IM using the structuring element SE, where SE is returned by STREL.
<i>numel()</i>	Number of elements in an array or subscripted array expression. N = numel(A) returns the number of elements, N, in array A.
<i>imreconstruct()</i>	Perform morphological reconstruction.
<i>size()</i>	Size of array.
<i>im2double()</i>	Convert image to double precision. Im2double takes an image as input, and returns an image of class double. If the input image is of class double, the output image is identical to it. If the input image is of class logical, uint8 or uint16, im2double returns the equivalent image of class double, rescaling or offsetting the data as necessary.
<i>watershed()</i>	Find image watershed regions.
<i>Bwmorph()</i>	Perform morphological operations on binary image.
<i>imcomplement()</i>	Complement image.
<i>sqrt()</i>	Find the square root
<i>bwdist()</i>	Distance transform. D = bwdist(BW) computes the Euclidean distance transform of the binary image BW. For each pixel in BW, the distance transform assigns a number that is the distance between that pixel and the nearest nonzero pixel of BW. bwdist uses the Euclidean distance metric by default. BW can have any dimension. D is the same size as BW.
<i>fspecial()</i>	fspecial Create 2-D special filters. H = fspecial(TYPE) creates a two-dimensional filter H of the specified type like averaging, sobel, perwit filters

APPENDIX III Source Code for Image Segmentation Algorithms

Please check the CD attached to the thesis report titled
Source code for
Image segmentation algorithms
Author: Mamata Naik
Date: July 2006
Department of Bioengineering, University of Strathclyde

An example of source code is shown below

THRESHOLDING

```
% Author - Naik M
% Date - July 2006 %
% Department of Bioengineering, University of Strathclyde
% This Program executes the thresholding method for an image segmentation. Thresholding, is the
% basic method which is used in Image segmentation technique.
% The program may take 4-5 minutes to run
%-----
% This Matlab® code is written in order to achieve Image thresholding using thresholding
% The programs involves two parts.
% Part A is thresholding code based on Local thresholding
% Part B is thresholding code based on Global Thresholding
%-----
% PART - A
% THRESHOLDING USING LOCAL THRESHOLDING
```

Intercomparison of image segmentation algorithms

```
%-----  
%      Some of the important Matlab® functions used in the part A are  
%      1. min  2. mean  3. abs  4. im2bw  5. strel  
%-----  
%      The following steps are being performed :  
%      1. The image is read into the Matlab® using the function 'imread'  
%      2. The image is then converted into gray scale using the function 'rgb2gray'  
%      3. The mean and the median for the image is calculated using the % functions max,min, mean  
%      4. Then the threshold is found using the equation  $T = (\text{mean} + \text{median}) / 2$ , where T= Threshold  
%      5. If the value of the pixel is greater or equal to the value of threshold,  
%      then the pixel is assigned the value 'one' else it is 'zero'  
%      6. The original and the thresholded images are displayed  
%-----  
%      input_image is the input image  
%      Thresh is the Threshold value  
%      Thresh_val is the value obtained after computing mean and the median  $T = (\text{mean} + \text{median}) / 2$   
%      output_image is the output image obtained after thresholding  
%-----  
glob_thresh                                % threshold value is stored in glob_thresh  
  
output_img=im2bw(filt_img,glob_thresh);    % im2bw produces binary images from indexed,  
                                           % intensity, or RGB images. To do this, it converts the  
                                           %input image to grayscale format (if it is not already  
                                           %an intensity image), and then converts this  
                                           % grayscale image to binary by thresholding.
```

*Refer the source code for complete program

APPENDIX IV COTENTS OF CD

Accompanying Compact Disc (CD) contains the following directories and files.

Directory	Files
Report	Thesis report
Presentations	Poster Presentation
	Thesis objective
Matlab codes	Thresholding
	Region growing
	FCM
	Watershed
	Non brain region removal
	Normalization
	Quantitative comparison

APPENDIX V A Short Note on the Project Work

1. Complete list of preprocessing algorithms which were developed and used

Preprocessing Algorithm used is the non-brain region removal using Morphological operators.

2. Complete list of all the segmentation algorithms which were developed and used.

1. Thresholding – Using both Local thresholding and global thresholding.
2. Region growing.
3. Morphological segmentation- using Watershed transforms.
4. Fuzzy-C-Means Algorithm.

3. Description, including source, of real and synthetic images which you used.

Synthetic images: Source: McConnell Brain Imaging Centre, Brain Web, Simulated brain database ⁷.

Types of images that were used are mentioned in the table below

T1-weighted 1mm slice thickness, 0% noise, 0% intensity non-uniformity
T2-weighted 1mm slice thickness, 0% noise, 0% intensity non-uniformity
PD image 1mm slice thickness, 0% noise, 0% intensity non-uniformity
T1 –weighted image with 7% noise, 20% RF inhomogeneity
T2 –weighted image with 7% noise, 20% RF inhomogeneity
PD –weighted image with 7% noise, 20% RF inhomogeneity

Real images: Source: Honark, Basics of MRI⁴⁴

4. A short description of the main input to your project, algorithms that were developed, testing that was carried out to ensure algorithms functioned correctly, data sets that were generated for algorithm evaluation.

Input to my project:

- Studying different algorithms.

Intercomparison of image segmentation algorithms

- Developing a few segmentation algorithms using Matlab[®].
- Testing algorithms on synthetic and real images.
- Qualitative and quantitative evaluation of algorithms.

Algorithms developed: 1. Thresholding 2. Region growing; 3. Morphological Segmentation 4. FCM Algorithm.

Testing: To ensure that that algorithms functioned correctly they were applied on a variety of synthetic images. In synthetic images the ground truth is known.

Data sets: For Qualitative evaluation: Prior Knowledge, Manual Interaction, Computational Method, Ability to segment regions, Noise, Spatial characteristics of an image.

For quantitative evaluation Histogram of the each original simulated image and each segmented image was obtained separately to count the number of pixels in the original simulated image and its segmented images respectively. Number of pixels, which are segmented correctly in the particular cluster and the number of pixels which are segmented incorrectly were found. Since simulated images were used it was possible to know precisely the original segmentation region which each pixel in the various regions belongs.